

# Optimal Error Analysis of Channel Estimation for IRS-assisted MIMO Systems

Zhen Qin and Zhihui Zhu, *Member, IEEE*

**Abstract**—As intelligent reflecting surface (IRS) has emerged as a new and promising technology capable of configuring the wireless environment favorably, channel estimation for IRS-assisted multiple-input multiple-output (MIMO) systems has garnered extensive attention in recent years. While various algorithms have been proposed to address this challenge, there is a lack of rigorous theoretical error analysis. This paper aims to address this gap by providing theoretical guarantees in terms of stable recovery of channel matrices for noisy measurements. We begin by establishing the equivalence between IRS-assisted MIMO systems and a compact tensor train (TT)-based tensor-on-tensor (ToT) regression. Building on this equivalence, we then investigate the restricted isometry property (RIP) for complex-valued subgaussian measurements. Our analysis reveals that successful recovery hinges on the relationship between the number of user terminals (in the uplink scenario) or base stations (in the downlink scenario) and the number of time slots during which channel matrices remain invariant. Utilizing the RIP condition, we analyze the theoretical recovery error for the solution to a constrained least-squares optimization problem, including upper error bound and minimax lower bound, demonstrating that the error decreases inversely with the number of time slots and increases proportionally with the number of unknown elements in the channel matrices. In addition, we extend our error analysis to two more specialized IRS-assisted MIMO systems, incorporating low-rank channel matrices or an unknown IRS. Furthermore, we explore a multi-hop IRS scheme and analyze the corresponding recovery errors. Finally, we introduce and implement two nonconvex optimization algorithms—alternating least squares and alternating gradient descent—to validate our conclusions through simulations.

**Index Terms**—Intelligent reflecting surface, restricted isometry property, error analysis, tensor train-based tensor-on-tensor regression.

## I. INTRODUCTION

IN a typical wireless propagation environment, transmitted signals undergo attenuation and scattering due to absorption, reflection, unexpected interference, diffraction, and refraction phenomena. Multipath propagation is generally acknowledged as a primary limiting factor in the performance of wireless communication systems [1]. While various physical layer techniques, such as advanced modulation/demodulation and precoding/decoding schemes, alongside the utilization of the mmWave/subTerahertz band, have been devised to counteract these adverse effects at the communication endpoints, it is evident that a plateau has been reached in terms of attainable data rates and performance reliability.

Considering the wireless environment as an additional variable for optimization holds the promise of significant performance gains. This promise is realized through the innovative concept of intelligent reflecting surface (IRS) [2]–[9], which can dynamically reshape the wireless propagation environment to exhibit more desirable characteristics. An IRS is essentially a 2D surface composed of numerous tunable units, which can be implemented using cost-effective antennas or metamaterials and controlled in real-time to manipulate communication channels without emitting signals of their own. Recently, IRS-assisted communications have garnered significant attention [10], owing to their potential to enhance efficiency, communication range, and capacity in wireless communication systems. Nevertheless, to fulfill the role of an IRS and achieve efficient and dependable wireless communication, the acquisition of precise channel state information using channel estimation techniques is imperative, posing a formidable challenge. One particular hurdle stems from the assumption that an IRS typically comprises passive elements, thereby necessitating the receiver to estimate the cascaded channel based on pilots transmitted by the transmitter through the IRS. Recently, numerous matrix-based methods for channel estimation [11]–[24] have been proposed and demonstrated commendable performance in practical implementation.

Building on these advancements, another promising approach leverages tensor models for channel estimation. Various tensor-based wireless communication systems, including mmWave [25]–[28] and IRS-assisted [29]–[33] multiple-input multiple-output (MIMO) models, have been developed, providing a concise framework for channel estimation. These models aim to accommodate diverse factors like spatial, temporal, spectral, coding, and polarization diversities. Compared to matrix-based models, tensor-based models offer greater flexibility in design, allowing for more effective exploitation of the inherent tensor structure, which can lead to improved recovery accuracy. The canonical polyadic (CP) decomposition [34] was initially applied in the IRS-assisted MIMO model [29]–[31] for its compact representation. To convert the optimization problem into a CP factorization problem, an orthogonal pilot signal matrix is assumed, and the IRS-assisted MIMO system needs to satisfy a coefficient constraint, ensuring the uniqueness of factor identification. Due to the lack of efficient and quasi-optimal decomposition methods, the alternating least squares method is commonly employed to tackle this challenge. On the other hand, since CP decomposition combined with an identity tensor can be viewed as a special case of the Tucker decomposition [35], [33] constructed a Tucker-based IRS-assisted MIMO model and applied a quasi-optimal method—Higher Order Singular Value

ZQ and ZZ are with the Department of Computer Science and Engineering, Ohio State University, Columbus, Ohio 43201, USA. (e-mail: {qin.660,zhu.3440}@osu.edu). This work was supported by NSF Grant CCF-2241298 and ECCS-2409701. We thank the Ohio Supercomputer Center for providing the computational resources needed in carrying out this work.

Decomposition—to achieve efficient channel estimation.

Although various optimization algorithms for IRS-assisted MIMO systems have demonstrated excellent performance, existing analyses of stable recovery focus solely on the required number of time slots by exploiting the uniqueness of solutions in matrix-based models [36] or the uniqueness conditions of tensor decompositions [30]. Despite these advances, there is no comprehensive error analysis for channel estimation in IRS-assisted MIMO systems, leading to the following critical question:

**Question:** What is the optimal recovery error for the channel estimation of the IRS-assisted MIMO system?

**Our contribution:** In this paper, we affirmatively address the main question through error analyses in the tensor-based multiple-access/multi-user IRS-assisted MIMO system. Instead of using CP or Tucker decompositions, we first rigorously establish that the combination of channel matrices and IRS is equivalent to the tensor train (TT) format [37], which has been extensively utilized in quantum physics for efficiently representing quantum states [38]–[40]. Additionally, we demonstrate that the IRS-assisted MIMO model aligns with the tensor-on-tensor (ToT) regression model [41]–[43] without any assumptions regarding the pilot signals. This mode extends the classical matrix/tensor regression framework, in which the response is the vector [44]–[49], to accommodate transmitted signals (represented by the second word “tensor” in the name) and the received signals (represented by the second word “tensor” in the name) as tensors. Building on the definitions outlined above, the channel estimation in a standard IRS-assisted MIMO model can be equivalently viewed as a recovery problem within the TT-based ToT regression model. Importantly, while other matrix/tensor-based models can be equivalently transformed into this framework, the TT-based ToT regression model is particularly advantageous because its canonical TT format [50, Theorem 1] facilitates theoretical analysis and the ToT model provides a compact representation that streamlines the design of optimization methods tailored to various pilot signal configurations. Consequently, this paper primarily focuses on analyzing this model.

Building on the previous discussion, our problem is reformulated as a recovery problem within the TT-based ToT regression model, representing a multiple-access/multi-user MIMO communication system assisted by an IRS in an uplink communication scenario. Towards that goal, we initially establish the restricted isometry property (RIP) for complex-valued subgaussian measurements, where each pilot signal element is a complex-valued subgaussian random variable. This analysis reveals an optimal size relationship between user terminals (UTs) and time slots. Notably, for a downlink communication scenario, RIP relates to base stations (BSs) and time slots. Subsequently, we investigate channel matrices recovery of the least square optimization problem from subgaussian measurements and derive recovery bounds relative to the number of time slots. Our findings illustrate that recovery error is inversely proportionate to the number of time slots, and successful recovery depends on the relationship between

UTs and time slots. Aside from aforementioned constraints, our recovery analyses remain free from other coefficient constraints. Moreover, we extend recovery error considerations to include low-rank channel matrices [30] and unknown IRS [51]. Next, we explore a multi-hop IRSs scheme and analyze corresponding recovery errors, laying the groundwork for future multi-hop IRSs communication design. Finally, we propose two nonconvex optimization algorithms—alternating least squares and alternating gradient descent and simulations affirm the validity of theoretical analyses.

**Notations** We use calligraphic letters (e.g.,  $\mathcal{Y}$ ) to denote tensors, bold capital letters (e.g.,  $\mathbf{Y}$ ) to denote matrices, except for  $\mathbf{X}_i$  which denotes the  $i$ -th order-3 tensor factors in the TT format ( $i = 2, \dots, N + M - 1$ ), bold lowercase letters (e.g.,  $\mathbf{y}$ ) to denote vectors, and italic letters (e.g.,  $y$ ) to denote scalar quantities.  $a^*$  is the complex conjugate of  $a$ . Elements of matrices and tensors are denoted in parentheses, as in Matlab notation. For example,  $\mathcal{X}(s_1, s_2, s_3)$  denotes the element in position  $(s_1, s_2, s_3)$  of the order-3 tensor  $\mathcal{X}$ . The inner product of  $\mathcal{A} \in \mathbb{R}^{d_1 \times \dots \times d_N}$  and  $\mathcal{B} \in \mathbb{R}^{d_1 \times \dots \times d_N}$  can be denoted as  $\langle \mathcal{A}, \mathcal{B} \rangle = \sum_{s_1=1}^{d_1} \dots \sum_{s_N=1}^{d_N} \mathcal{A}(s_1, \dots, s_N) \mathcal{B}(s_1, \dots, s_N)$ .  $\|\mathcal{X}\|_F = \sqrt{\langle \mathcal{X}, \mathcal{X} \rangle}$  is the Frobenius norm of  $\mathcal{X}$ . Tensor contraction is defined as  $\mathcal{A} \times_i^j \mathcal{B}$  of size  $d_1 \times \dots \times d_{i-1} \times d_{i+1} \times \dots \times d_N \times h_1 \times \dots \times h_{j-1} \times h_{j+1} \times \dots \times h_M$  with  $(s_1, \dots, s_{i-1}, s_{i+1}, \dots, s_N, f_1, \dots, f_{j-1}, f_{j+1}, \dots, f_M)$ -th entry being  $\sum_k \mathcal{A}(s_1, \dots, s_{i-1}, k, s_{i+1}, \dots, s_N) \mathcal{B}(f_1, \dots, f_{j-1}, k, f_{j+1}, \dots, f_M)$  for  $\mathcal{A} \in \mathbb{R}^{d_1 \times \dots \times d_{i-1} \times d_k \times d_{i+1} \times \dots \times d_N}$  and  $\mathcal{B} \in \mathbb{R}^{h_1 \times \dots \times h_{j-1} \times d_k \times h_{j+1} \times \dots \times h_M}$ . The procedure of  $\mathcal{A} \times_{i_1, \dots, i_n}^{j_1, \dots, j_n} \mathcal{B}$  can be viewed as a sequence of  $n$  tensor contractions  $\mathcal{A} \times_{i_k}^{j_k} \mathcal{B}, k \in [n]$ .  $\|\mathbf{X}\|$  represents the spectral norm of the matrix  $\mathbf{X}$ . For a positive integer  $K$ ,  $[K]$  denotes the set  $\{1, \dots, K\}$ . For two positive quantities  $a, b \in \mathbb{R}$ , the inequality  $b = O(a)$  means  $b \leq ca$  for some universal constant  $c$ ; likewise,  $b = \Omega(a)$  indicates that  $b \geq ca$  for some universal constant  $c$ .

## II. SINGLE-HOP IRS-ASSISTED MIMO SYSTEM

**Model formulation** We consider a multiple-access/multi-user MIMO communication system assisted by an IRS, in which the  $P$  base stations (BSs) receive the signals transmitted by  $U$  user terminals (UTs) via the IRS. The terminology employed in this paper is based on an uplink communication scenario, where the transmitter is referred to as the UT and the receiver as the BS. However, it is important to note that our signal model and theoretical analysis can be equally applied to the downlink case by merely reversing the roles of the transmitter and the receiver. Without loss of generality, we assume that each BS and each UT are equipped with the same number of antennas, denoted as  $L$  and  $M$  respectively. The IRS is composed of  $N$  passive elements, or unit cells, capable of individually adjusting their reflection coefficients (i.e., phase shifts). Due to unfavorable propagation conditions, BS-UT channels are neglected [29]. We also assume quasi-static flat fading channel model, where all the channels remain invariant during  $T$  time slots. Assuming a block-fading channel, the received signal model is usually given as follows [15,29]–[31]

$$\mathbf{y}(t) = \mathbf{H} \text{diag}(s(t)) \mathbf{G} \mathbf{x}(t) + \mathbf{w}(t), \quad t \in [T], \quad (1)$$

where the IRS-BS channel is  $\mathbf{H} = [\mathbf{H}_1^\top \cdots \mathbf{H}_P^\top]^\top \in \mathbb{C}^{LP \times N}$  in which  $\mathbf{H}_p \in \mathbb{C}^{L \times N}$ ,  $p \in [P]$  is the  $p$ -th IRS-BS channel, and the UT-IRS channel is  $\mathbf{G} = [\mathbf{G}_1 \cdots \mathbf{G}_U] \in \mathbb{C}^{N \times UM}$  in which  $\mathbf{G}_u \in \mathbb{C}^{N \times M}$ ,  $u \in [U]$  is  $u$ -th the UT-IRS channel.  $\mathbf{x}(t) = [\mathbf{x}_1^\top(t) \cdots \mathbf{x}_U^\top(t)]^\top \in \mathbb{C}^{UM \times 1}$  is the vector containing the transmitted pilot signals at time  $t$ , where  $\mathbf{x}_u(t) \in \mathbb{C}^{M \times 1}$  is the  $u$ -th user pilot vector. The phase shift vector at time  $t$  is defined as  $\mathbf{s}(t) = [s_1(t)e^{j\phi_1(t)} \cdots s_N(t)e^{j\phi_N(t)}]^\top \in \mathbb{C}^{N \times 1}$ , where  $s_n(t) \in \{0, 1\}$  and  $e^{j\phi_n(t)} \in (0, 2\pi]$  represent the on or off state and the phase shift of the  $n$ -th IRS element at time instant  $t$ , respectively.  $\mathbf{w}(t) \sim \mathcal{CN}(\mathbf{0}, \gamma^2 \mathbf{I}_{LP})$  denotes the complex additive white Gaussian noise (AWGN).

The channel coherence time  $T_s$  is divided into  $K$  blocks, where each block has  $T$  time slots so that  $T_s = KT$  [29]. Let us define  $\mathbf{y}(k, t) = \mathbf{y}((k-1)T + t)$  as the received signal at the  $t$ -th time slot of the  $k$ -th block, where  $t \in [T]$  and  $k \in [K]$ . In addition, we denote  $\mathbf{x}(k, t)$  and  $\mathbf{s}(k, t)$  as the pilot signal and phase shift vectors associated with the  $t$ -th time slot of the  $k$ -th block. In each block, the user transmits the same pilot signal and the IRS phase shift vector is invariant, but the phase shift vector between blocks is changeable, which means that the IRS has  $K$  phase configurations. Consequently, we have  $\mathbf{s}(k) = \mathbf{s}(k, t)$  and  $\mathbf{x}(t) = \mathbf{x}(k, t)$ . The received signal is given by

$$\mathbf{y}(k, t) = \mathbf{H} \text{diag}(\mathbf{s}(k)) \mathbf{G} \mathbf{x}(t) + \mathbf{w}(k, t), \quad t \in [T] \text{ and } k \in [K].$$

By respectively stacking  $\mathbf{y}(k, t)$ ,  $\mathbf{x}(t)$  and  $\mathbf{w}(k, t)$ ,  $t \in [T]$  into matrices  $\mathbf{Y}(k) = [\mathbf{y}(k, 1) \cdots \mathbf{y}(k, T)] \in \mathbb{C}^{LP \times T}$ ,  $\mathbf{X} = [\mathbf{x}(1) \cdots \mathbf{x}(T)] \in \mathbb{C}^{UM \times T}$  and  $\mathbf{W}(k) = [\mathbf{w}(k, 1) \cdots \mathbf{w}(k, T)] \in \mathbb{C}^{LP \times T}$ , we have

$$\mathbf{Y}(k) = \mathbf{H} \text{diag}(\mathbf{s}(k)) \mathbf{G} \mathbf{X} + \mathbf{W}(k). \quad (2)$$

The objective is to estimate the channel matrices  $\mathbf{H}$  and  $\mathbf{G}$  from the received signals  $\{\mathbf{Y}(k)\}_{k=1}^K$  by appropriately designing the pilot signal matrix  $\mathbf{X}$  and the phase shift vectors  $\{\mathbf{s}(k)\}_{k=1}^K$ . Notably, this formulation highlights (i) the flexibility in designing  $\mathbf{X}$  to optimize estimation performance, and (ii) the desire to minimize the number of time slots  $T$  to enhance efficiency.

Previous studies [13,29]–[31,52] have reformulated (2) as a noisy CP factorization problem. This is achieved either by treating  $\mathbf{G}\mathbf{X}$  as a single matrix [29,30,52] under the assumption that the pseudoinverse of  $\mathbf{X}$  exists, or by assuming that the pilot signal matrix  $\mathbf{X}$  is orthogonal [13,31], such as employing the discrete Fourier transform (DFT) matrix, allowing (2) to be rewritten as  $\mathbf{Y}(k)\mathbf{X}^H = \mathbf{H} \text{diag}(\mathbf{s}(k)) \mathbf{G} + \mathbf{W}(k)\mathbf{X}^H$ . However, these assumptions impose constraints on the design of the pilot signal matrix, limiting their applicability to general cases. Moreover, the CP factorization framework used for single-hop IRS-assisted MIMO systems does not readily extend to multi-hop configurations, presenting additional challenges.

**Compact tensor representation** To accommodate a more general setting for the pilot signal matrix  $\mathbf{X}$ , we can reinterpret (2) as a tensor-on-tensor (ToT) regression model. Specifically, by aggregating the received data over  $K$  blocks, we can define three tensors as  $\mathcal{Y} \in \mathbb{C}^{LP \times K \times T}$ ,  $\mathcal{S} \in \mathbb{C}^{N \times K \times N}$  and  $\mathcal{W} \in \mathbb{C}^{LP \times K \times T}$ , where  $\mathcal{Y}(:, k, :) = \mathbf{Y}(k)$ ,  $\mathcal{S}(:, k, :) = \text{diag}(\mathbf{s}(k))$

and  $\mathcal{W}(:, k, :) = \mathbf{W}(k)$ . Then, the ground-truth channel tensor  $\mathcal{B}^* \in \mathbb{C}^{LP \times K \times UM}$  can be defined as follows:

$$\begin{aligned} \mathcal{B}^*(p, k, m) &= \mathbf{H}(p, :) \mathcal{S}(:, k, :) \mathbf{G}(:, m) \\ &= \mathbf{H}(p, :) \text{diag}(\mathbf{s}(k)) \mathbf{G}(:, m). \end{aligned} \quad (3)$$

Compared to directly analyzing (2), the tensor formulation enables the modeling of correlations in the signal model (2) across different phase configurations indexed by  $k$ . Thus, each element of  $\mathcal{Y}$  can be represented as

$$\mathcal{Y}(p, k, t) = \sum_{m=1}^{UM} \mathcal{B}^*(p, k, m) \mathbf{X}(m, t) + \mathcal{W}(p, k, t). \quad (4)$$

In this context,  $\mathcal{Y}$  and  $\mathbf{X}$  represent the first and second tensors in the ‘‘tensor-on-tensor’’ regression model<sup>1</sup>, respectively. It is evident that the pilot signal (measurement operator)  $\mathbf{X}$  exclusively affects UTs, as the received signal  $\mathcal{Y}$  is a tensor of size  $LP \times K \times T$  and the channel tensor  $\mathcal{B}^*$  in (4) is a tensor of size  $LP \times K \times UM$ , implying the total number of antennas in the UTs  $UM$  should be contingent on the number of time slots  $T$ .

Notice that, unlike the construction of CP decomposition, which requires transforming (3) as demonstrated in [13,29]–[31,52], (3) is inherently represented in the standard tensor train (TT) format as each element of  $\mathcal{B}^*$  can be expressed in a matrix product form (a detailed introduction to the TT decomposition is provided in Appendix A). By applying the tensor contraction operation [53], the TT form of  $\mathcal{B}^*$  can be expressed as:

$$\mathcal{B}^* = [\mathbf{H}, \mathcal{S}, \mathbf{G}] = \mathbf{H} \times_2^1 \mathcal{S} \times_3^1 \mathbf{G} \in \mathbb{C}^{LP \times K \times UM}, \quad (5)$$

where  $(\mathbf{H} \times_2^1 \mathcal{S})(p, k, i) = \sum_{n=1}^N \mathbf{H}(p, n) \mathcal{S}(n, k, i)$  and  $(\mathcal{C} \times_3^1 \mathbf{G})(p, k, m) = \sum_{n=1}^N \mathcal{C}(p, k, n) \mathbf{G}(n, m)$ .

Therefore, we can rewrite (4) as a TT-based ToT regression model.

$$\begin{aligned} \mathcal{Y} &= \mathcal{X}(\mathcal{B}^*) + \mathcal{W} = \mathcal{B}^* \times_3^1 \mathbf{X} + \mathcal{W} \\ &= [\mathbf{H}, \mathcal{S}, \mathbf{G}] \times_3^1 \mathbf{X} + \mathcal{W}, \end{aligned} \quad (6)$$

where  $(\mathcal{B}^* \times_3^1 \mathbf{X})(p, k, t) = \sum_{j=1}^{UM} \mathcal{B}^*(p, k, j) \mathbf{X}(j, t)$ . The linear map  $\mathcal{X}(\mathcal{B}^*) : \mathbb{C}^{LP \times K \times UM} \rightarrow \mathbb{C}^{LP \times K \times T}$  models the measurement process.

We now consider minimizing the following constrained least squares objective to recover the channel tensor  $\mathcal{B}^*$ :

$$\hat{\mathcal{B}} = \arg \min_{\mathcal{B} \in \mathbb{B}_{N,S}} \frac{1}{T} \|\mathcal{X}(\mathcal{B}) - \mathcal{Y}\|_F^2, \quad (7)$$

where we define a set of order-3 TT format tensor as following:

$$\begin{aligned} \mathbb{B}_{N,S} &= \{\mathcal{B} = [\mathbf{H}, \mathcal{S}, \mathbf{G}] : \mathbf{H} \in \mathbb{C}^{LP \times N}, \mathbf{G} \in \mathbb{C}^{N \times UM} \\ &\text{are unknown and } \mathcal{S} \in \mathbb{C}^{N \times K \times N} \text{ is known}\}. \end{aligned} \quad (8)$$

The advantage of the least-squares formulation is that it allows the application of well-established tools from standard matrix/tensor regression models, such as the Restricted Isometry Property (RIP) condition [40,54]–[57], as detailed in the following discussion. Subsequently, we provide a rigorous theoretical analysis, deriving error bounds for channel estimation.

<sup>1</sup>Without loss of generality, we can regard the matrix  $\mathbf{X}$  as an order-2 tensor.

**Error analysis** One advantage of viewing the channel estimation as the regression model is that analogous to the analysis in standard matrix/tensor regression models, a larger number of time slots  $T$  tends to enhance denoising effectiveness since the error bound of channel estimation in the IRS-assisted MIMO model should heavily rely on  $T$ . Recently, we analyzed the statistical guarantee of the TT-based ToT regression model in [58]. However, these results cannot be directly applied to the IRS-assisted MIMO model because recovery errors pertain to the entire tensor recovery. Since the phase shift tensor  $\mathcal{S}$  is often known, only the channel matrices are affected by noise. Consequently, the recovery error should be primarily related to the channel matrices. Next, we will establish the upper bound and the minimax lower bound of the recovery error for channel estimation.

To facilitate the recovery of channels  $\mathbf{H}$  and  $\mathbf{G}$  from their linear measurements  $\mathcal{Y}$ , the pilot signal (regression/measurement operator) need adhere to specific properties. One such desirable property is the RIP, extensively explored and popularized in compressive regression literature [54]–[56,59]. This property has also been extended to structured tensors [40,57].

**Theorem 1.** *Suppose each element of the pilot signal matrix  $\mathbf{X}$  is a complex-valued subgaussian random variable<sup>2</sup>. Let  $\delta_{UM} \in (0, 1)$  be a positive constant. Then, for any channel tensor  $\mathcal{B} \in \mathbb{B}_{N,S}$ , when the number of time slots satisfies*

$$T \geq C \cdot \frac{UM}{\delta_{UM}^2}, \quad (9)$$

with probability  $1 - e^{-cT}$ ,  $\mathcal{X}$  satisfies the  $UM$ -RIP:

$$(1 - \delta_{UM})\|\mathcal{B}\|_F^2 \leq \frac{1}{T}\|\mathcal{X}(\mathcal{B})\|_F^2 \leq (1 + \delta_{UM})\|\mathcal{B}\|_F^2, \quad (10)$$

where  $c$  and  $C$  are positive constants.

The proof is presented in Appendix B. Theorem 1 guarantees the RIP for subgaussian measurement ensembles, with the number of time slots  $T$  scaling linearly only in relation to the total number of antennas ( $UM$ ) in the UTs<sup>3</sup>. Subgaussian random variables, including Gaussian, Bernoulli, PSK, QAM, and PAM signals, can be conveniently designed as pilot signals in practical applications. Notably, while each element of the Haar-distributed random unitary matrix is a subgaussian random variable, the same does not hold for the elements of the normalized DFT matrix,  $\frac{1}{\sqrt{T}}\mathbf{X}$ , a commonly employed pilot signal matrix. Nevertheless, the DFT matrix satisfies (10)

<sup>2</sup>Note that a complex-valued random variable  $X$  is subgaussian if and only if its both real part  $\text{Re}\{X\}$  and imaginary part  $\text{Im}\{X\}$  are real subgaussian random variables. Here are some classical examples of subgaussian distributions.

- (Gaussian) A standard complex Gaussian random variable  $X = \text{Re}\{X\} + i\text{Im}\{X\}$  with  $\text{Re}\{X\}$  and  $\text{Im}\{X\}$  being independent and following  $\mathcal{N}(0, \frac{1}{2})$ , is a subgaussian random variable.
- (Bernoulli) A Bernoulli random variable  $X$  that takes values  $-1$  and  $1$  with equal probability is a subgaussian random variable.
- (Digital modulation signals) The phase shift keying (PSK) [60], quadrature amplitude modulation (QAM) [61] and pulse amplitude modulation (PAM) [62] exhibit subgaussian random variable properties.

<sup>3</sup>In a downlink communication scenario, the parameter  $T$  will be connected to the total number of antennas ( $LP$ ) in the BSs.

when  $T \geq UM$ , rendering the subsequent conclusions with  $\delta_{UM} = 0$  applicable to them as well. Our analysis centers on the subgaussian case to streamline the discussion. When RIP holds, then for any two distinct TT format channel tensors  $\mathcal{B}_1, \mathcal{B}_2 \in \mathbb{B}_{N,S}$ , noting that  $\mathcal{B}_1 - \mathcal{B}_2 \in \mathbb{B}_{2N,S}$  is also a TT format channel tensor according to (30) in Appendix A, we have distinct measurements since

$$\begin{aligned} \frac{1}{T}\|\mathcal{X}(\mathcal{B}_1) - \mathcal{X}(\mathcal{B}_2)\|_F^2 &= \frac{1}{T}\|\mathcal{X}(\mathcal{B}_1 - \mathcal{B}_2)\|_F^2 \\ &\geq (1 - \delta_{UM})\|\mathcal{B}_1 - \mathcal{B}_2\|_F^2, \end{aligned} \quad (11)$$

which guarantees the possibility of exact recovery of channel matrices in the channel tensor.

Next, we present a formal analysis of the upper bound for  $\|\hat{\mathcal{B}} - \mathcal{B}^*\|_F$  with  $\hat{\mathcal{B}} \in \mathbb{B}_{N,S}$ . Here, we provide a concise summary of the main result.

**Theorem 2.** *(Upper bound of  $\|\hat{\mathcal{B}} - \mathcal{B}^*\|_F$ ) Given a channel tensor  $\mathcal{B}^*$  in (8) where  $\mathbf{H}$  and  $\mathbf{G}$  are full rank, when each element of the pilot signal matrix  $\mathbf{X}$  is a complex-valued subgaussian random variable and each element in  $\mathcal{W}$  follows the complex normal distribution  $\mathcal{CN}(0, \gamma^2)$ , with probability  $1 - 2e^{-c_1(LP+UMN)}$  for a positive constant  $c_1$ , we have*

$$\|\hat{\mathcal{B}} - \mathcal{B}^*\|_F \leq O\left(\frac{\gamma\sqrt{(1 + \delta_{UM})(LPN + UMN)}}{(1 - \delta_{UM})\sqrt{T}}\right), \quad (12)$$

where  $\hat{\mathcal{B}}$  is the solution to (7).

The detailed analysis is provided in Appendix C. Theorem 2 guarantees a stable recovery of the ground truth  $\mathcal{B}^*$  when the number of time slots  $T$  is linearly proportionate to  $LPN + UMN$ . Combining the condition  $T \geq \Omega(UM/\delta_{UM}^2)$  in (9) with  $\|\hat{\mathcal{B}} - \mathcal{B}^*\|_F \leq \epsilon$ , the number of time slots  $T$  should satisfy

$$T \geq \max\left\{\Omega\left(\frac{UM}{\delta_{UM}^2}\right), \Omega\left(\frac{(1 + \delta_{UM})(LPN + UMN)\gamma^2}{(1 - \delta_{UM})^2\epsilon^2}\right)\right\}$$

to ensure a small recovery error.

Next we consider two special cases: (i) Theorem 2 assumes that the channel matrices  $\mathbf{H}$  and  $\mathbf{G}$  are full rank, but in some scenarios, such as millimeter-wave MIMO systems, the presence of a large number of transmit/receive antennas combined with scattering-poor propagation may lead to low-rank channel matrices  $\mathbf{H}$  and  $\mathbf{G}$  [15,63]. When the signal travels between the BS and IRS across  $r_1$  clusters, and between the IRS and the UT across  $r_2$  clusters, it is reasonable to assume that  $\mathbf{H}$  is a rank- $r_1$  matrix and  $\mathbf{G}$  is a rank- $r_2$  matrix. By leveraging the covering number of low-rank matrices as introduced in [64, Lemma 3.1] and applying it to (40) in Appendix C, we can readily extend (12) to

$$\begin{aligned} \|\hat{\mathcal{B}} - \mathcal{B}^*\|_F \\ \leq O\left(\frac{\gamma\sqrt{(1 + \delta_{UM})((LP + N)r_1 + (UM + N)r_2)}}{(1 - \delta_{UM})\sqrt{T}}\right), \end{aligned} \quad (13)$$

where  $\hat{\mathcal{B}}, \mathcal{B}^* \in \{\mathcal{B} = [\mathbf{H}, \mathcal{S}, \mathbf{G}] : \mathbf{H} \in \mathbb{C}^{LP \times N}$  with  $\text{rank}(\mathbf{H}) = r_1, \mathbf{G} \in \mathbb{C}^{N \times UM}$  with  $\text{rank}(\mathbf{G}) = r_2, \text{ are unknown and } \mathcal{S} \in \mathbb{C}^{N \times K \times N}$  is known\}. It is important to note that a

comparison between (12) and (13) reveals that the improvement in recovery error due to low-rankness occurs only when  $r_1 \leq \frac{LPN}{LP+N}$  and  $r_2 \leq \frac{UMN}{UM+N}$ .

(ii) It is crucial to emphasize that the elements of the IRS in outdoor scenarios, being exposed to weather and atmospheric conditions, may encounter unknown blockages and time-dependent fluctuations in their phase and amplitude responses [51]. Consequently, the IRS tensor  $\mathcal{S}$  deviates from its intended structure, and the assumption of perfect knowledge of all phase shifts at the receiver may not be valid in such cases. To analyze the scenario where  $\mathcal{S}$  is unknown, by introducing the covering number for  $\mathcal{S}$  to the proof in Appendix C, we can obtain

$$\|\widehat{\mathcal{B}} - \mathcal{B}^*\|_F \leq O\left(\frac{\gamma\sqrt{(1+\delta_{UM})(LPN+KN+UMN)}}{(1-\delta_{UM})\sqrt{T}}\right),$$

where  $\widehat{\mathcal{B}}, \mathcal{B}^* \in \{\mathcal{B} = [\mathbf{H}, \mathcal{S}, \mathbf{G}] : \mathbf{H} \in \mathbb{C}^{LP \times N}, \mathcal{S} \in \mathbb{C}^{N \times K \times N}, \mathbf{G} \in \mathbb{C}^{N \times UM} \text{ are unknown}\}$ . Apart from the additional term  $KN$ , this upper bound closely aligns with (12). Hence, we omit redundant discussions and concentrate exclusively on the scenario where  $\mathcal{S}$  is perfectly known.

Our second goal is to establish a minimax lower bound using Gaussian ensemble design. This lower bound proves to be a valuable tool for gaining insights into the parameters that influence the achievable error of a given problem. Furthermore, it reveals that the upper bound in (12) is tight and optimal. Following the derivation in Appendix D, we arrive at:

**Theorem 3.** (Minimax lower bound of  $\|\widehat{\mathcal{B}} - \mathcal{B}^*\|_F$ ) *In the context of the TT-based ToT regression model in (6), we assume a channel tensor  $\mathcal{B}^*$  from (8), where  $\mathbf{H}$  and  $\mathbf{G}$  are full rank and  $N \geq C'$  with  $C'$  being a universal constant. Assuming each element of  $\mathbf{X}$  and  $\mathcal{W}$  in (6) follows  $\mathcal{CN}(0, 1)$  and  $\mathcal{CN}(0, \gamma^2)$ , respectively, we obtain:*

$$\inf_{\widehat{\mathcal{B}}} \sup_{\mathcal{B}^* \in \mathbb{B}_{N, \mathcal{S}}} \mathbb{E} \|\widehat{\mathcal{B}} - \mathcal{B}^*\|_F \geq \Omega\left(\sqrt{\frac{LPN+UMN}{T}}\gamma\right). \quad (14)$$

Note that the constraint  $N \geq C'$  is not strictly necessary, primarily simplifying the theoretical analysis in Appendix D.

### III. GENERALIZATION TO MULTI-HOP IRS-ASSISTED MIMO SYSTEM

The preceding section focuses on the single-hop IRS assisted MIMO system, recognized as a promising technology to address the propagation distance challenge [6,65]–[68]. However, in specific scenarios like urban areas or satellite-to-indoor communications, employing a multi-hop IRSs scheme becomes imperative to surmount severe signal blockage between BSs and UTs for enhanced service coverage [69]–[71]. Furthermore, in the context of Terahertz (0.1-10 THz) band communication, considered a promising technology for achieving ultra-high speed and low-latency communications, deploying multiple passive IRSs between BSs and UTs proves effective in overcoming inherent propagation attenuations.

**Tensor-based model formulation** In this section, we explore the  $D$ -IRS scheme connecting UTs and BSs, assuming unavailability of channels from UT to BS, from UT to the  $i$ -th IRS ( $1 < i \leq D$ ), from the  $j$ -th IRS ( $1 \leq j < D$ )

to BS, and between non-adjacent IRSs due to blockage or excessive path loss. In detail, we denote the UT-1-th IRS channel as  $\mathbf{B}_0 \in \mathbb{C}^{N_1 \times UM}$ , the  $D$ -th IRS-BS channel as  $\mathbf{B}_D \in \mathbb{C}^{LP \times N_D}$ , the channel from the  $d$ -th IRS to the  $(d+1)$ -th IRS as  $\mathbf{B}_d \in \mathbb{C}^{N_{d+1} \times N_d}$  for  $d \in [D-1]$ , and represent the  $d$ -th IRS as  $\mathcal{S}_d \in \mathbb{C}^{N_d \times K \times N_d}$  for  $d \in [D]$ . Here,  $\mathcal{S}_d(:, k, :) = \text{diag}(\mathbf{s}_d(k)) \in \mathbb{C}^{N_d \times N_d}$ , and the design of  $\mathbf{s}_d(k)$  is same with (2). We define each element of the channel tensor  $\mathcal{B}_D^* \in \mathbb{C}^{LP \times K \times UM}$  as follows:

$$\mathcal{B}_D^*(p, k, j) = \mathbf{B}_D(p, :) \Pi_{d=1}^{D-1} \mathcal{S}_{d+1}(:, k, :) \mathbf{B}_d \cdot \mathcal{S}_1(:, k, :) \mathbf{B}_0(:, j). \quad (15)$$

Assume that each element of  $\mathcal{W}$  is subject to complex additive white Gaussian noise, the received signal is given by

$$\widetilde{\mathcal{Y}}(p, k, t) = \sum_{j=1}^{UM} \mathcal{B}_D^*(p, k, j) \mathbf{X}(j, t) + \mathcal{W}(p, k, t), \quad (16)$$

where, in contrast to the multi-hop scheme [69], we assume the absence of a direct channel from the BS to the UT to streamline the analysis.

Note that each element  $\mathcal{B}_D^*(p, k, j)$  can still be conceptualized as an element of an order- $2D+1$  TT format tensor due to its multiplication form resembling (29). Specifically, to establish a connection between the channel tensor  $\mathcal{B}_D^*$  and the TT format tensor, we can reinterpret  $\mathbf{B}_d \in \mathbb{C}^{N_{d+1} \times N_d}$  as an order-3 tensor  $\widetilde{\mathbf{B}}_d \in \mathbb{C}^{N_{d+1} \times 1 \times N_d}$ . Accordingly, we define  $\widehat{\mathcal{B}}_D^*$  as the result of a sequence of tensor contractions<sup>4</sup>:  $\mathbf{B}_D \times_2 \mathcal{S}_D \times_3 \widetilde{\mathbf{B}}_{D-1} \times_4 \cdots \times_2 \widetilde{\mathbf{B}}_1 \times_2 \mathcal{S}_1 \times_2 \mathbf{B}_0$ . As a result,  $\widehat{\mathcal{B}}_D^*$  can be represented as an order- $2D+1$  TT format tensor with dimensions  $LP \times K \times 1 \times K \times \cdots \times 1 \times K \times UM$  with TT ranks<sup>5</sup>  $(N_D, N_D, N_{D-1}, N_{D-1}, \dots, N_1, N_1)$ . Further insights can be gained, revealing that

$$\mathcal{B}_D^*(p, k, j) = \begin{cases} \widehat{\mathcal{B}}_D^*(p, k_1, 1, k_2, 1, \dots, k_D, j), & k_1 = \cdots = k_D = k, \\ 0, & \text{otherwise,} \end{cases} \quad (17)$$

where it becomes evident that  $\mathcal{B}_D^*$  emerges as a sampled outcome of  $\widehat{\mathcal{B}}_D^*$ . To streamline the notation, we introduce the notation  $\mathcal{B}_D^* = [\mathbf{B}_D, \mathcal{S}_D, \mathbf{B}_{D-1}, \dots, \mathcal{S}_1, \mathbf{B}_0] \in \mathbb{C}^{LP \times K \times UM}$ . Consequently, we define the TT-based ToT regression model as following:

$$\begin{aligned} \widetilde{\mathcal{Y}} &= \mathcal{X}(\mathcal{B}_D^*) + \mathcal{W} = \mathcal{B}_D^* \times_3 \mathbf{X} + \mathcal{W} \\ &= [\mathbf{B}_D, \mathcal{S}_D, \mathbf{B}_{D-1}, \dots, \mathcal{S}_1, \mathbf{B}_0] \times_3 \mathbf{X} + \mathcal{W}. \end{aligned} \quad (18)$$

Now, we consider the following constrained least squares objective:

$$\widehat{\mathcal{B}}_D = \arg \min_{\mathcal{B}_D \in \mathbb{B}_{N, \{\mathcal{S}_i\}}^D} \frac{1}{T} \|\mathcal{X}(\mathcal{B}_D) - \widetilde{\mathcal{Y}}\|_F^2, \quad (19)$$

<sup>4</sup>Here, the tensor contraction operation  $\mathcal{A}_1 \times_d \mathcal{A}_2$  for  $\mathcal{A}_1 \in \mathbb{C}^{N_1 \times \cdots \times N_D}$  and  $\mathcal{A}_2 \in \mathbb{C}^{N_1 \times M_2 \times M_3}$  results in a new tensor  $\mathcal{A}_3$  of size  $N_1 \times \cdots \times N_{d-1} \times N_{d+1} \times \cdots \times N_D \times M_2 \times M_3$ , with the  $(n_1, \dots, n_{d-1}, n_{d+1}, \dots, n_D, m_2, m_3)$ -th element being  $\sum_{n_d} \mathcal{A}_1(n_1, \dots, n_d) \mathcal{A}_2(n_d, m_2, m_3)$ .

<sup>5</sup>The definition of TT ranks is provided in Appendix A.

where we define the set of  $\mathbb{B}_{N,\{\mathcal{S}_i\}}^D$  as follows:

$$\begin{aligned} \mathbb{B}_{N,\{\mathcal{S}_i\}}^D = \{ & \mathcal{B}_D = [\mathbf{B}_D, \mathcal{S}_D, \dots, \mathbf{B}_1, \mathcal{S}_1, \mathbf{B}_0] \in \mathbb{C}^{LP \times K \times UM} : \\ & \mathbf{B}_D \in \mathbb{C}^{LP \times N_D}, \mathbf{B}_0 \in \mathbb{C}^{N_1 \times UM}, \mathbf{B}_d \in \mathbb{C}^{N_{d+1} \times N_d}, \\ & d \in [D-1] \text{ are unknown and } \mathcal{S}_d \in \mathbb{C}^{N_d \times K \times N_d}, \\ & d \in [D] \text{ are known} \}, \end{aligned} \quad (20)$$

in which  $N = \max_d N_d$ . Note that each element of  $\mathcal{B}_D$  follows (15). In the subsequent section, we present a comprehensive error analysis of the channel estimation process.

**Error analysis** Before presenting the error analysis, we first ensure that the measurements satisfy the RIP condition. By following a similar derivation as provided in Appendix B, the RIP condition for  $\mathcal{X}(\mathcal{B}_D)$  can be directly obtained.

**Theorem 4.** *Suppose each element of the pilot signal matrix  $\mathbf{X}$  is a complex-valued subgaussian random variable. Let  $\delta_{UM} \in (0, 1)$  be a positive constant. Then, for any channel tensor  $\mathcal{B}^D \in \mathbb{B}_{N,\{\mathcal{S}_i\}}^D$ , when the number of time slots satisfies*

$$T \geq C \cdot \frac{UM}{\delta_{UM}^2}, \quad (21)$$

with probability  $1 - e^{-cT}$ ,  $\mathcal{X}$  satisfies the UM-RIP:

$$(1 - \delta_{UM}) \|\mathcal{B}_D\|_F^2 \leq \frac{1}{T} \|\mathcal{X}(\mathcal{B}_D)\|_F^2 \leq (1 + \delta_{UM}) \|\mathcal{B}_D\|_F^2, \quad (22)$$

where  $c$  and  $C$  is a universal constant.

Similar to Theorem 1, Theorem 4 ensures that the number of time slots is solely contingent upon the total number of antennas (UM) in the UTs. This is attributed to the fact that the pilot signal matrix  $\mathbf{X}$  is exclusively associated with the UT-1-th IRS channel  $\mathbf{B}_0$ . Then we can further analyze the recovery error  $\|\hat{\mathcal{B}}_D - \mathcal{B}_D^*\|_F$ .

**Theorem 5.** *(Upper bound of  $\|\hat{\mathcal{B}}_D - \mathcal{B}_D^*\|_F$ ) Given a channel tensor  $\mathcal{B}_D^*$  in (20) in which  $\mathbf{B}_d, d = 0, \dots, D$  are full rank, when each element of the pilot signal matrix  $\mathbf{X}$  is a complex-valued subgaussian random variable and each element in  $\mathcal{W}$  follows the complex normal distribution  $\mathcal{CN}(0, \gamma^2)$ , with probability  $1 - 2e^{-c_1(\sum_{d=0}^D N_d N_{d+1}) \log D}$  for a positive constant  $c_1$ , we have*

$$\|\hat{\mathcal{B}}_D - \mathcal{B}_D^*\|_F \leq O\left(\frac{\gamma \sqrt{(1 + \delta_{UM})(\sum_{d=0}^D N_d N_{d+1}) \log D}}{(1 - \delta_{UM})\sqrt{T}}\right), \quad (23)$$

where  $N_0 = UM$ ,  $N_{D+1} = LP$  and  $\hat{\mathcal{B}}_D$  is the solution to (19).

The proof has been provided in Appendix E. Theorem 5 ensures an optimal recovery error bound, given that the degree of freedom for the unknown variables in (19) is  $O(LP N_D + UM N_1 + \sum_{i=1}^{D-1} N_d N_{d+1})$ . However, it is noteworthy that while increasing the number of IRSs can expand service coverage, the recovery error of channel estimation may also increase when the number of time slots  $T$  is limited. Therefore, in practical implementation, a balance should be struck between service coverage and recovery error. Similar to the analysis of the minimax lower bound using the Gaussian

ensemble design in Theorem 3, this result can also be extended to multi-hop IRS-assisted MIMO systems.

**Theorem 6.** *(Minimax lower bound of  $\|\hat{\mathcal{B}}_D - \mathcal{B}_D^*\|_F$ ) In the context of the TT-based ToT regression model in (18), we assume a channel tensor  $\mathcal{B}_D^*$  from (20), where  $\mathbf{B}_d, d = 0, \dots, D$  are full rank and  $\min N_d \geq C'$  with  $C'$  being a universal constant. Assuming each element of  $\mathbf{X}$  and  $\mathcal{W}$  in (6) follows  $\mathcal{CN}(0, 1)$  and  $\mathcal{CN}(0, \gamma^2)$ , respectively, we obtain:*

$$\inf_{\hat{\mathcal{B}}_D} \sup_{\mathcal{B}_D^* \in \mathbb{B}_{N,\{\mathcal{S}_i\}}^D} \mathbb{E} \|\hat{\mathcal{B}}_D - \mathcal{B}_D^*\|_F \geq \Omega\left(\sqrt{\frac{\sum_{d=0}^D N_d N_{d+1}}{T}} \gamma\right). \quad (24)$$

Finally, akin to the analysis of a single-hop IRS-assisted MIMO system, it is imperative to address the following two special cases. (i) First, when  $\mathbf{B}_d, d = 0, \dots, D$  are rank- $r_d$  matrices, by incorporating the covering number of low-rank matrices into (60) in Appendix E, we can derive

$$\begin{aligned} & \|\hat{\mathcal{B}}_D - \mathcal{B}_D^*\|_F \\ & \leq O\left(\frac{\gamma \sqrt{(1 + \delta_{UM})(\sum_{d=0}^D (N_d + N_{d+1}) r_d) \log D}}{(1 - \delta_{UM})\sqrt{T}}\right), \end{aligned}$$

where  $\hat{\mathcal{B}}_D, \mathcal{B}_D^* \in \{\mathcal{B}_D = [\mathbf{B}_D, \mathcal{S}_D, \dots, \mathbf{B}_1, \mathcal{S}_1, \mathbf{B}_0] \in \mathbb{C}^{LP \times K \times UM} : \mathbf{B}_D \in \mathbb{C}^{LP \times N_D}, \mathbf{B}_0 \in \mathbb{C}^{N_1 \times UM}, \mathbf{B}_d \in \mathbb{C}^{N_{d+1} \times N_d}, d \in [D-1] \text{ are unknown with } \text{rank}(\mathbf{B}_d) = r_d, d = 0, \dots, D, \text{ and } \mathcal{S}_d \in \mathbb{C}^{N_d \times K \times N_d}, d \in [D] \text{ are known}\}$ . Leveraging low-rank structures offers a potential avenue for improving error performance, as the recovery error may be reduced below (23) when the ranks  $r_d, d = 0, \dots, D$  are small.

(ii) Second, when  $\mathcal{S}_i, i \in [D]$ , are unknown, introducing the covering number of  $\{\mathcal{S}_i\}_{i=1}^D$  into the proof in Appendix E, similar to (23), we can arrive at

$$\begin{aligned} & \|\hat{\mathcal{B}}_D - \mathcal{B}_D^*\|_F \\ & \leq O\left(\frac{\gamma \sqrt{(1 + \delta_{UM})(\sum_{d=0}^D N_d N_{d+1} + \sum_{d=1}^D K N_d) \log D}}{(1 - \delta_{UM})\sqrt{T}}\right), \end{aligned}$$

where  $\hat{\mathcal{B}}_D, \mathcal{B}_D^* \in \{\mathcal{B}_D = [\mathbf{B}_D, \mathcal{S}_D, \dots, \mathbf{B}_1, \mathcal{S}_1, \mathbf{B}_0] \in \mathbb{C}^{N_{D+1} \times K \times N_0} : \mathbf{B}_d \in \mathbb{C}^{N_{d+1} \times N_d}, d = 0, \dots, D, \mathcal{S}_d \in \mathbb{C}^{N_d \times K \times N_d}, d \in [D] \text{ are unknown}\}$ . In this analysis, we assume that all IRSs are equipped with active elements. However, in practice, when adjustments are required for only a subset of IRSs, denoted as  $\mathcal{S}_i$  for  $i \in \Omega$ , where  $\Omega \subseteq \{1, \dots, D\}$ , the recovery error can be further reduced. Specifically, the term  $\sum_{d=1}^D K N_d$  is replaced by  $\sum_{i \in \Omega} K N_i$ .

**Discussion** Beyond the IRS-assisted MIMO system, the tensor-based ToT model can also be effectively applied to a variety of typical communication systems, including direct-sequence code-division multiple-access systems [72], space-time frequency MIMO systems [73], and cooperative/relay systems [74,75]. Compared with traditional representations, tensor-based methods offer a more compact and efficient form for modeling and processing. Furthermore, by following the same analytical approach above, the optimal recovery error for channel estimation in these systems can be derived, as it is proportionate to the degrees of freedom of the channel

matrices, assuming the RIP condition is satisfied using certain transmitted pilot signals. These results offer a theoretical guarantee for robustness and potential accuracy in estimating channel characteristics.

#### IV. NONCONVEX OPTIMIZATION ALGORITHMS

In this section, our focus will be on designing algorithms for estimating the channel matrices within the framework of the TT-based ToT regression model. Initially, we will concentrate on the single-hop IRS-assisted MIMO system and subsequently extend our approach to the multi-hop IRS-assisted MIMO system. Note that, given that the following algorithms can be readily extended to handle the unknown  $\mathcal{S}$  scenario, our attention is directed towards the known  $\mathcal{S}$  case at the receiver.

**Single-hop IRS-assisted MIMO system** (i) One common assumption is that the pilot signal matrix  $\mathbf{X}$  is a truncated discrete Fourier transform (DFT) matrix or a semi-unitary matrix, as discussed in previous works [13,31]. However, we can extend this assumption by considering the existence of the pseudoinverse for  $\mathbf{X}$ . Expanding upon the equivalent form of the TT format  $\mathcal{B} = [\mathbf{H}, \mathcal{S}, \mathbf{G}]$  [76], denoted as  $\mathcal{B}^{(1)} = \mathbf{H}R(\mathcal{S})(\mathbf{G} \otimes \mathbf{I}_K)$  and  $\mathcal{B}^{(2)} = (\mathbf{I}_K \otimes \mathbf{H})L(\mathcal{S})\mathbf{G}$  (The expressions for  $L(\mathcal{S})$  and  $R(\mathcal{S})$  are provided in (31) and (32) of Appendix A.)<sup>6</sup>, we can formulate the following loss function:

$$\min_{\widehat{\mathbf{H}} \in \mathbb{C}^{LP \times N}} \|\widehat{\mathbf{H}}R(\mathcal{S})(\widehat{\mathbf{G}} \otimes \mathbf{I}_K) - (\mathcal{Y} \times_3 \mathbf{X}^\dagger)^{(1)}\|_F^2, \quad (25)$$

$$\min_{\widehat{\mathbf{G}} \in \mathbb{C}^{N \times UM}} \|(\mathbf{I}_K \otimes \widehat{\mathbf{H}})L(\mathcal{S})\widehat{\mathbf{G}} - (\mathcal{Y} \times_3 \mathbf{X}^\dagger)^{(2)}\|_F^2. \quad (26)$$

Specifically, we apply the following alternating least squares (ALS) algorithm:

$$\begin{aligned} \mathbf{H}^{(l+1)} &= (\mathcal{Y} \times_3 \mathbf{X}^\dagger)^{(1)}(R(\mathcal{S})(\mathbf{G}^{(l)} \otimes \mathbf{I}_K))^\dagger, \\ \mathbf{G}^{(l+1)} &= ((\mathbf{I}_K \otimes \mathbf{H}^{(l+1)})L(\mathcal{S}))^\dagger(\mathcal{Y} \times_3 \mathbf{X}^\dagger)^{(2)}. \end{aligned}$$

To guarantee the existence of all pseudoinverse matrices, it is imperative that the conditions  $N \leq \min\{UMK, LPK\}$  and  $T \geq UM$  are met but we note that  $N \leq \min\{UMK, LPK\}$  is a sufficient condition, not a necessary one. This is because Theorem 2 holds for all coefficients when  $T \geq \Omega(UM)$ . Additionally, when  $\mathbf{H}$  and  $\mathbf{G}$  exhibit low-rank characteristics, we can employ SVD to truncate small singular values, facilitating the use of low-rank projection in each iteration.

(ii) To address the numerical stability challenges of the pseudoinverse and to accommodate a broader class of pilot signal matrices  $\mathbf{X}$ , we can alternatively optimize the following loss function directly:

$$\min_{\substack{\widehat{\mathbf{H}} \in \mathbb{C}^{LP \times N} \\ \widehat{\mathbf{G}} \in \mathbb{C}^{N \times UM}}} f(\widehat{\mathbf{H}}, \widehat{\mathbf{G}}) = \frac{1}{T} \|\mathcal{X}([\widehat{\mathbf{H}}, \mathcal{S}, \widehat{\mathbf{G}}]) - \mathcal{Y}\|_F^2. \quad (27)$$

<sup>6</sup>Let  $\mathcal{X}^{(i)} \in \mathbb{C}^{(d_1 \cdots d_i) \times (d_{i+1} \cdots d_N)}$  denote the  $i$ -th unfolding matrix of the tensor  $\mathcal{X} \in \mathbb{C}^{d_1 \times \cdots \times d_N}$ . The  $(s_1 \cdots s_i, s_{i+1} \cdots s_N)$ -th element of  $\mathcal{X}^{(i)}$  is given by  $\mathcal{X}^{(i)}(s_1 \cdots s_i, s_{i+1} \cdots s_N) = \mathcal{X}(s_1, \dots, s_N)$ . Here,  $s_1 \cdots s_i$  and  $s_{i+1} \cdots s_N$  represent the row and column indices, respectively, where the row index is calculated as  $s_1 + d_1(s_2 - 1) + \cdots + d_1 \cdots d_{i-1}(s_i - 1)$  and the column index as  $s_{i+1} + d_{i+1}(s_{i+2} - 1) + \cdots + d_{i+1} \cdots d_{N-1}(s_N - 1)$ .

As for (27), we solve the above optimization problem by the following alternating gradient descent (AGD):

$$\begin{aligned} \mathbf{H}^{(l+1)} &= \mathbf{H}^{(l)} - \mu \nabla_{\mathbf{H}^*} f(\mathbf{H}^{(l)}, \mathbf{G}^{(l)}), \\ \mathbf{G}^{(l+1)} &= \mathbf{G}^{(l)} - \mu \nabla_{\mathbf{G}^*} f(\mathbf{H}^{(l+1)}, \mathbf{G}^{(l)}), \end{aligned}$$

where  $\mu$  is a step size and we define the Wirtinger gradients  $\nabla_{\mathbf{H}^*} f(\mathbf{H}^{(l)}, \mathbf{G}^{(l)})$  and  $\nabla_{\mathbf{G}^*} f(\mathbf{H}^{(l+1)}, \mathbf{G}^{(l)})$  as follows:

$$\begin{aligned} \nabla_{\mathbf{H}^*} f(\mathbf{H}^{(l)}, \mathbf{G}^{(l)}) &= \frac{1}{T} ((\mathcal{B}^{(l)} \times_3 \mathbf{X} - \mathcal{Y}) \times_3^2 \mathbf{X}^*) \\ &\quad \times_{2,3}^{2,3} (\mathcal{S}^* \times_3^1 (\mathbf{G}^{(l)})^*), \\ \nabla_{\mathbf{G}^*} f(\mathbf{H}^{(l+1)}, \mathbf{G}^{(l)}) &= \frac{1}{T} ((\mathbf{H}^{(l+1)})^* \times_2^1 \mathcal{S}^*) \\ &\quad \times_{1,2}^{1,2} ((\mathcal{B}^{(l)} \times_3 \mathbf{X} - \mathcal{Y}) \times_3^2 \mathbf{X}^*). \end{aligned}$$

In comparison to the ALS algorithm, the AGD does not require additional coefficient constraints, aside from the condition  $T \geq \Omega(UM)$  for satisfying the RIP condition. Additionally, it avoids the numerical stability issues associated with the pseudoinverse.

**Multi-hop IRS-assisted MIMO system** In a multi-hop IRS-assisted MIMO system, where channel matrices and IRSs are represented in (20), a closed-form solution for the ALS method is not feasible. Consequently, we primarily consider the AGD method and the following loss function:

$$\begin{aligned} &\arg \min_{\substack{\widehat{\mathbf{B}}_D \in \mathbb{C}^{LP \times ND}, \widehat{\mathbf{B}}_0 \in \mathbb{C}^{N_1 \times UM}, \\ \widehat{\mathbf{B}}_d \in \mathbb{C}^{N_{d+1} \times Nd}, d \in [D-1]}} g(\widehat{\mathbf{B}}_D, \dots, \widehat{\mathbf{B}}_0) \\ &= \frac{1}{T} \|\mathcal{X}([\widehat{\mathbf{B}}_D, \mathcal{S}_D, \dots, \widehat{\mathbf{B}}_1, \mathcal{S}_1, \widehat{\mathbf{B}}_0]) - \widetilde{\mathcal{Y}}\|_F^2. \quad (28) \end{aligned}$$

We solve this nonconvex optimization problem by the following AGD algorithm for  $d = 0, \dots, D$ :

$$\mathbf{B}_d^{(l+1)} = \mathbf{B}_d^{(l)} - \mu \nabla_{\mathbf{B}_d^*} g(\mathbf{B}_D^{(l+1)}, \dots, \mathbf{B}_{d+1}^{(l+1)}, \mathbf{B}_d^{(l)}, \dots, \mathbf{B}_0^{(l)}),$$

where  $\mu$  is a step size and the Wirtinger gradient  $\nabla_{\mathbf{B}_d^*} g(\mathbf{B}_D, \dots, \mathbf{B}_0)$  is defined as:

$$\begin{aligned} \nabla_{\mathbf{B}_d^*} g(\mathbf{B}_D, \dots, \mathbf{B}_0) &= \frac{1}{T} \sum_{k=1}^K \mathcal{S}_{d+1}^H(:, k, :) \mathbf{B}_{d+1}^H \cdots \\ &\quad \mathcal{S}_D^H(:, k, :) \mathbf{B}_D^H \left( \mathcal{X}([\mathbf{B}_D, \mathcal{S}_D(:, k, :), \dots, \mathbf{B}_1, \mathcal{S}_1(:, k, :), \right. \\ &\quad \left. \mathbf{B}_0]) - \widetilde{\mathcal{Y}}(:, k, :) \right) \mathbf{X}^H \mathbf{B}_0^H \cdots \mathbf{B}_{d-1}^H \mathcal{S}_d^H(:, k, :). \end{aligned}$$

In line with the single-hop IRS-assisted MIMO system, AGD in this scenario similarly operates without coefficient constraints, except for the condition  $T \geq \Omega(UM)$  for satisfying the RIP condition.

We note that for low-rank channel estimation, iterative hard thresholding combined with truncated singular value decomposition [77] can be effectively integrated into the AGD method.

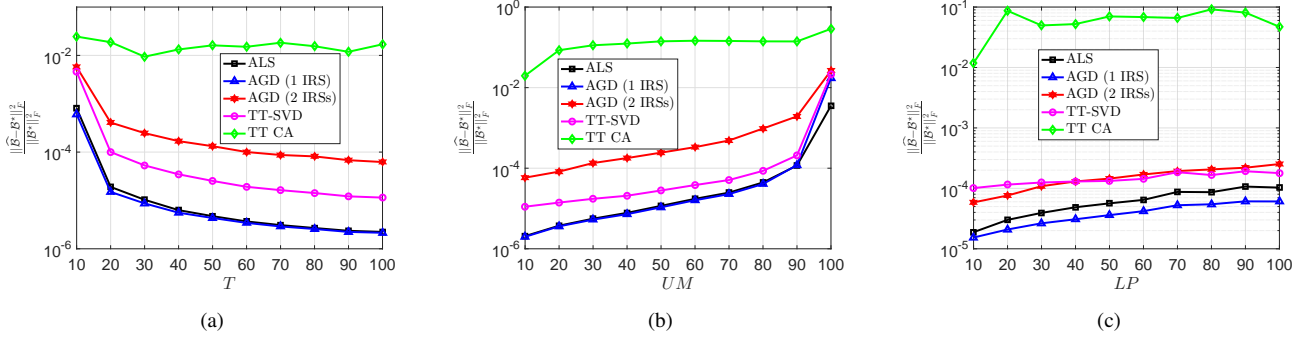


Fig. 1. Recovery performance for channel matrices (a) for different  $T$  with  $UM = LP = K = N = 10$  and  $\gamma^2 = 10^{-6}$ , (b) for different  $UM$  with  $T = 100$ ,  $LP = K = N = 10$  and  $\gamma^2 = 10^{-6}$ , (c) for different  $LP$  with  $T = 20$ ,  $UM = K = N = 10$  and  $\gamma^2 = 10^{-6}$ .

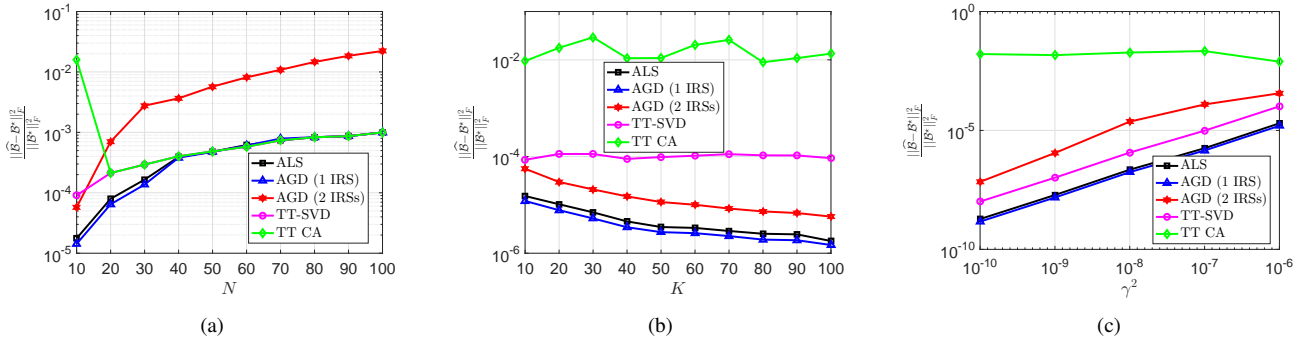


Fig. 2. Recovery performance for channel matrices (a) for different  $N$  with  $T = 20$ ,  $UM = LP = K = 10$  and  $\gamma^2 = 10^{-6}$ , (b) for different  $K$  with  $T = 20$ ,  $UM = LP = N = 10$  and  $\gamma^2 = 10^{-6}$ ,  $\mu = 0.02$  for the 1 IRS scenario and  $\mu = 0.1$  for the 2 IRSs scenario, (c) for different  $\gamma^2$  with  $T = 20$  and  $UM = LP = K = N = 10$ .

## V. EXPERIMENTAL RESULTS

In this section, we conduct numerical experiments to evaluate the effectiveness of Theorem 2 and Theorem 5. We consider 1 IRS and 2 IRSs assisted MIMO systems, where each element of channel matrices  $\mathbf{H}$ ,  $\mathbf{G}$ ,  $\mathbf{B}_0$ ,  $\mathbf{B}_1$ ,  $\mathbf{B}_2$ , and pilot signal matrix  $\mathbf{X}$  follows independent and identically complex standard normal distribution. Subsequently, we normalize the above channel matrices to have a unit Frobenius norm. To effectively estimate the channel matrices in the 1 IRS assisted MIMO system, we apply the ALS, AGD, tensor train singular value decomposition (TT-SVD) [37], and tensor train cross-approximation (TT CA) via the greedy restricted cross-interpolation (GRCI) algorithm [78]. As two representative methods for TT decomposition, TT-SVD and TT-CA are employed for the tensor factorization of  $\mathcal{Y} \times_3 \mathbf{X}^\dagger$ . In the case of the 2 IRSs model, we employ the AGD algorithm. We initialize ALS and AGD with random matrices, with elements generated from a complex standard normal distribution. To simplify parameter selection and notation in the 2 IRSs system, we set  $N_1 = N_2 = N$  and denote  $\mathcal{B}_2 = \mathcal{B}$ ,  $\mathcal{B}_2^* = \mathcal{B}^*$ . The number of iterations for the ALS, AGD (1 IRS), and AGD (2 IRSs) algorithms are set to 100,  $10^5$ , and  $2 \times 10^5$ , respectively. For the AGD algorithm, we set  $\mu = 0.2$  for the 1 IRS scenario and  $\mu = 1$  for the 2 IRSs scenario. For each experimental setting, we conduct 20 Monte Carlo trials and then take the average over the 20 trials to report the results.

In the first experiment, we compare the recovery performance of different methods with various values of  $T$ ,  $UM$ , and  $LP$  in Figure 1. These plots illustrate that the recovery error tends to decrease with larger values of  $T$ , or smaller values of  $UM$  and  $LP$ , consistent with our theoretical findings presented in Theorem 2 and Theorem 5. Additionally, we observe the following: (i) when  $T$  approaches  $UM$ , the recovery error could worsen since RIP conditions (9) and (21) are not satisfied; (ii) AGD (1 IRS) and ALS exhibit similar recovery performance except for when  $T = UM$ ; (iii) the recovery error of AGD (2 IRSs) is larger than AGD (1 IRS) due to the introduction of an additional channel matrix, leading to more error as shown in Theorem 5; (iv) compared to the ALS and AGD algorithms, TT-SVD and TT CA demonstrate poorer recovery performance. This is because TT-SVD and TT CA do not utilize the known information of  $\mathcal{S}$  or  $\mathcal{S}_i$ ,  $i = 1, 2$ , resulting in a larger error. Furthermore, the recovery error of TT-CA is larger than that of TT-SVD, as TT-SVD utilizes the full information of the channel tensor, whereas TT-CA does not [79]; (v) from Figure 1(c), it is evident that successful recovery is not dependent on  $LP$ , as even with  $LP = 100$ , the recovery remains stable when  $T = 20$ .

In the second experiment, we examine the recovery performance of different methods across varying values of  $N$  and  $K$ . Keeping a fixed number of time slots  $T = 20$ , we observe stable recovery errors with increasing  $N$  and  $K$ . However, it is noteworthy that as  $K$  increases, the recovery



performance generally improves, except for TT-SVD and TT CA. This is attributed to the fact that the coherence time  $T_s = KT$  becomes larger as  $K$  increases while  $T$  remains fixed, thereby enhancing performance. However, factorization approaches like TT-SVD and TT CA struggle to effectively denoise as  $K$  increases. This is due to the possibility that the estimated  $\hat{\mathcal{S}}$  or  $\hat{\mathcal{S}}_1, \hat{\mathcal{S}}_2$  may introduce more noise under these conditions. This highlights a limitation of tensor factorization in recovering channel matrices of IRS-based systems.

In the third experiment, we compare the recovery performance of different methods across various noise variances  $\gamma^2$ . In Figure 2(c), we observe that, except for TT CA, the recovery error exhibits a linear relationship with  $\gamma^2$ , consistent with the analysis in Theorem 2 and Theorem 5. Ultimately, while the ALS achieves performance similar to the AGD, the AGD may offer greater stability, especially in time-varying systems where the pseudoinverse of the input matrix may not be well-defined.

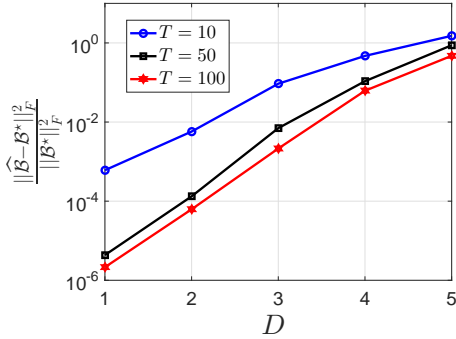


Fig. 3. Recovery performance for channel matrices for different  $D$  with  $K = N_0 = \dots = N_D = 10$ ,  $\gamma^2 = 10^{-6}$  and  $\mu$  sequentially selected from the set  $\{0.2, 1, 5, 10, 15\}$ .

In the final experiment, we compare the recovery performance of AGD for different numbers of IRSs  $D$ . As shown in Section V, the recovery error increases linearly with  $D$ , aligning with the theoretical analysis in Theorem 5. Additionally, as  $T$  increases, the recovery error decreases. Thus, for fixed  $T$  time slots, a trade-off emerges between mitigating propagation attenuations with multiple IRSs and minimizing recovery error.

## VI. CONCLUSION

This paper addresses the significant gap in theoretical error analysis concerning channel estimation for IRS-assisted MIMO systems. By establishing the equivalence between these systems and tensor train-based tensor-on-tensor (ToT) regression, we provide insights into the fundamental factors crucial for the successful recovery of channel matrices. Our analysis highlights the pivotal role of the relationship between the number of user terminals or base stations and the number of time slots for ensuring stable recovery. Furthermore, we extend our investigation to consider low-rank channel matrices and unknown IRS, enhancing the applicability of our findings. Additionally, through our exploration of a multi-hop IRS scheme, we evaluate corresponding recovery errors,

shedding light on the performance of such configurations. Finally, to validate our theoretical conclusions, we propose and implement two nonconvex optimization algorithms—alternating least squares and alternating gradient descent—demonstrating their effectiveness through experimental results.

An important area for future research involves conducting error analysis on two-way, two-hop IRS-assisted MIMO systems [80]–[82]. Unlike the one-way multi-hop IRS-assisted model discussed in this paper, the optimization problem in the two-way scenario, where channels between base stations/user terminals and IRSs are accessible, consists of two ToT regression problems. Thus, our current analytical approach cannot be directly extended to this setup. Furthermore, another challenging aspect for future investigation is the local convergence analysis and global geometry of the IRS-assisted optimization problem. Despite the promising experimental results obtained even with random initialization, unlike the rotation ambiguity commonly encountered in standard nonconvex matrix/tensor recovery [45]–[48], a diagonal (scaling) ambiguity exists between channel matrices, as noted in [36, Section 2]. This ambiguity poses a challenge in analyzing the optimization problem at hand.

## REFERENCES

- [1] T. Singal, *Wireless communications*. Tata McGraw-Hill Education, 2010.
- [2] W. Tang, M. Z. Chen, X. Chen, J. Y. Dai, Y. Han, M. Di Renzo, Y. Zeng, S. Jin, Q. Cheng, and T. J. Cui, “Wireless communications with reconfigurable intelligent surface: Path loss modeling and experimental measurement,” *IEEE Transactions on Wireless Communications*, vol. 20, no. 1, pp. 421–439, 2020.
- [3] X. Cao, B. Yang, H. Zhang, C. Huang, C. Yuen, and Z. Han, “Reconfigurable-intelligent-surface-assisted mac for wireless networks: Protocol design, analysis, and optimization,” *IEEE Internet of Things Journal*, vol. 8, no. 18, pp. 14 171–14 186, 2021.
- [4] E. Basar, M. Di Renzo, J. De Rosny, M. Debbah, M.-S. Alouini, and R. Zhang, “Wireless communications through reconfigurable intelligent surfaces,” *IEEE access*, vol. 7, pp. 116 753–116 773, 2019.
- [5] S. Gong, X. Lu, D. T. Hoang, D. Niyato, L. Shu, D. I. Kim, and Y.-C. Liang, “Toward smart wireless communications via intelligent reflecting surfaces: A contemporary survey,” *IEEE Communications Surveys & Tutorials*, vol. 22, no. 4, pp. 2283–2314, 2020.
- [6] C. Liaskos, S. Nie, A. Tsioliaridou, A. Pitsillides, S. Ioannidis, and I. Akyildiz, “A new wireless communication paradigm through software-controlled metasurfaces,” *IEEE Communications Magazine*, vol. 56, no. 9, pp. 162–169, 2018.
- [7] M. Jung, W. Saad, Y. Jang, G. Kong, and S. Choi, “Performance analysis of large intelligent surfaces (liss): Asymptotic data rate and channel hardening effects,” *IEEE Transactions on Wireless Communications*, vol. 19, no. 3, pp. 2052–2065, 2020.
- [8] C. Huang, A. Zappone, G. C. Alexandropoulos, M. Debbah, and C. Yuen, “Reconfigurable intelligent surfaces for energy efficiency in wireless communication,” *IEEE transactions on wireless communications*, vol. 18, no. 8, pp. 4157–4170, 2019.
- [9] E. Basar, “Reconfigurable intelligent surface-based index modulation: A new beyond mimo paradigm for 6g,” *IEEE Transactions on Communications*, vol. 68, no. 5, pp. 3187–3196, 2020.
- [10] M. Di Renzo, A. Zappone, M. Debbah, M.-S. Alouini, C. Yuen, J. De Rosny, and S. Tretyakov, “Smart radio environments empowered by reconfigurable intelligent surfaces: How it works, state of research, and the road ahead,” *IEEE journal on selected areas in communications*, vol. 38, no. 11, pp. 2450–2525, 2020.
- [11] X. Ma, Z. Chen, W. Chen, Z. Li, Y. Chi, C. Han, and S. Li, “Joint channel estimation and data rate maximization for intelligent reflecting surface assisted terahertz mimo communication systems,” *IEEE Access*, vol. 8, pp. 99 565–99 581, 2020.

- [12] B. Ning, Z. Chen, W. Chen, and Y. Du, "Channel estimation and transmission for intelligent reflecting surface assisted thz communications," in *ICC 2020-2020 IEEE International Conference on Communications (ICC)*. IEEE, 2020, pp. 1–7.
- [13] L. Wei, C. Huang, G. C. Alexandropoulos, and C. Yuen, "Parallel factor decomposition channel estimation in ris-assisted multi-user mimo communication," in *2020 IEEE 11th sensor array and multichannel signal processing workshop (SAM)*. IEEE, 2020, pp. 1–5.
- [14] T. L. Jensen and E. De Carvalho, "An optimal channel estimation scheme for intelligent reflecting surfaces based on a minimum variance unbiased estimator," in *ICASSP 2020-2020 IEEE International Conference on Acoustics, Speech and Signal Processing (ICASSP)*. IEEE, 2020, pp. 5000–5004.
- [15] Z.-Q. He and X. Yuan, "Cascaded channel estimation for large intelligent metasurface assisted massive mimo," *IEEE Wireless Communications Letters*, vol. 9, no. 2, pp. 210–214, 2019.
- [16] Y. Cui and H. Yin, "An efficient csi acquisition method for intelligent reflecting surface-assisted mmwave networks," *arXiv preprint arXiv:1912.12076*, 2019.
- [17] J. Chen, Y.-C. Liang, H. V. Cheng, and W. Yu, "Channel estimation for reconfigurable intelligent surface aided multi-user mmwave mimo systems," *IEEE Transactions on Wireless Communications*, 2023.
- [18] J. Mirza and B. Ali, "Channel estimation method and phase shift design for reconfigurable intelligent surface assisted mimo networks," *IEEE Transactions on Cognitive Communications and Networking*, vol. 7, no. 2, pp. 441–451, 2021.
- [19] S. Jeong, A. Farhang, N. S. Perović, and M. F. Flanagan, "Low-complexity joint cfo and channel estimation for ris-aided ofdm systems," *IEEE Wireless Communications Letters*, vol. 11, no. 1, pp. 203–207, 2021.
- [20] M.-M. Zhao, Q. Wu, M.-J. Zhao, and R. Zhang, "Exploiting amplitude control in intelligent reflecting surface aided wireless communication with imperfect csi," *IEEE Transactions on Communications*, vol. 69, no. 6, pp. 4216–4231, 2021.
- [21] H. Liu, X. Yuan, and Y.-J. A. Zhang, "Matrix-calibration-based cascaded channel estimation for reconfigurable intelligent surface assisted multiuser mimo," *IEEE Journal on Selected Areas in Communications*, vol. 38, no. 11, pp. 2621–2636, 2020.
- [22] Y. Jin, J. Zhang, X. Zhang, H. Xiao, B. Ai, and D. W. K. Ng, "Channel estimation for semi-passive reconfigurable intelligent surfaces with enhanced deep residual networks," *IEEE transactions on vehicular technology*, vol. 70, no. 10, pp. 11 083–11 088, 2021.
- [23] C. Hu, L. Dai, S. Han, and X. Wang, "Two-timescale channel estimation for reconfigurable intelligent surface aided wireless communications," *IEEE Transactions on Communications*, vol. 69, no. 11, pp. 7736–7747, 2021.
- [24] X. Hu, R. Zhang, and C. Zhong, "Semi-passive elements assisted channel estimation for intelligent reflecting surface-aided communications," *IEEE Transactions on Wireless Communications*, vol. 21, no. 2, pp. 1132–1142, 2021.
- [25] Z. Zhou, J. Fang, L. Yang, H. Li, Z. Chen, and S. Li, "Channel estimation for millimeter-wave multiuser mimo systems via parafac decomposition," *IEEE Transactions on Wireless Communications*, vol. 15, no. 11, pp. 7501–7516, 2016.
- [26] X. Wu, S. Ma, and X. Yang, "Tensor-based low-complexity channel estimation for mmwave massive mimo-ofds systems," *Journal of Communications and Information Networks*, vol. 5, no. 3, pp. 324–334, 2020.
- [27] Z. Zhou, J. Fang, L. Yang, H. Li, Z. Chen, and R. S. Blum, "Low-rank tensor decomposition-aided channel estimation for millimeter wave mimo-ofdm systems," *IEEE Journal on Selected Areas in Communications*, vol. 35, no. 7, pp. 1524–1538, 2017.
- [28] Y. Lin, S. Jin, M. Matthaiou, and X. You, "Tensor-based channel estimation for millimeter wave mimo-ofdm with dual-wideband effects," *IEEE Transactions on Communications*, vol. 68, no. 7, pp. 4218–4232, 2020.
- [29] G. T. de Araújo and A. L. de Almeida, "Parafac-based channel estimation for intelligent reflective surface assisted mimo system," in *2020 IEEE 11th Sensor Array and Multichannel Signal Processing Workshop (SAM)*. IEEE, 2020, pp. 1–5.
- [30] G. T. de Araújo, A. L. de Almeida, and R. Boyer, "Channel estimation for intelligent reflecting surface assisted mimo systems: A tensor modeling approach," *IEEE Journal of Selected Topics in Signal Processing*, vol. 15, no. 3, pp. 789–802, 2021.
- [31] X. Zhang, X. Shao, Y. Guo, Y. Lu, and L. Cheng, "Sparsity-structured tensor-aided channel estimation for ris-assisted mimo communications," *IEEE Communications Letters*, vol. 26, no. 10, pp. 2460–2464, 2022.
- [32] J. Du, Y. Cheng, L. Jin, and F. Gao, "Time-varying phase noise estimation, channel estimation, and data detection in ris-assisted mimo systems via tensor analysis," *IEEE Transactions on Signal Processing*, vol. 71, pp. 3426–3441, 2023.
- [33] P. R. Gomes, G. T. de Araújo, B. Sokal, A. L. de Almeida, B. Makki, and G. Fodor, "Channel estimation in ris-assisted mimo systems operating under imperfections," *IEEE Transactions on Vehicular Technology*, 2023.
- [34] R. Bro, "Parafac. Tutorial and applications," *Chemometrics and intelligent laboratory systems*, vol. 38, no. 2, pp. 149–171, 1997.
- [35] L. R. Tucker, "Some mathematical notes on three-mode factor analysis," *Psychometrika*, vol. 31, no. 3, pp. 279–311, 1966.
- [36] C. Pan, G. Zhou, K. Zhi, S. Hong, T. Wu, Y. Pan, H. Ren, M. Di Renzo, A. L. Swindlehurst, R. Zhang *et al.*, "An overview of signal processing techniques for ris/irs-aided wireless systems," *IEEE Journal of Selected Topics in Signal Processing*, 2022.
- [37] I. Oseledets, "Tensor-train decomposition," *SIAM Journal on Scientific Computing*, vol. 33, no. 5, pp. 2295–2317, 2011.
- [38] J. Eisert, M. Cramer, and M. B. Plenio, "Colloquium: Area laws for the entanglement entropy," *Reviews of modern physics*, vol. 82, no. 1, p. 277, 2010.
- [39] K. Noh, L. Jiang, and B. Fefferman, "Efficient classical simulation of noisy random quantum circuits in one dimension," *Quantum*, vol. 4, p. 318, 2020.
- [40] Z. Qin, C. Jameson, Z. Gong, M. B. Wakin, and Z. Zhu, "Quantum state tomography for matrix product density operators," *IEEE Transactions on Information Theory*, vol. 70, no. 7, pp. 5030–5056, 2024.
- [41] E. F. Lock, "Tensor-on-tensor regression," *Journal of Computational and Graphical Statistics*, vol. 27, no. 3, pp. 638–647, 2018.
- [42] G. Raskutti, M. Yuan, and H. Chen, "Convex regularization for high-dimensional multiresponse tensor regression," *The Annals of Statistics*, vol. 47, no. 3, pp. 1554–1584, 2019.
- [43] C. Llosa-Vite and R. Maitra, "Reduced-rank tensor-on-tensor regression and tensor-variate analysis of variance," *IEEE Transactions on Pattern Analysis and Machine Intelligence*, vol. 45, no. 2, pp. 2282–2296, 2022.
- [44] E. J. Candes and Y. Plan, "Tight oracle inequalities for low-rank matrix recovery from a minimal number of noisy random measurements," *IEEE Transactions on Information Theory*, vol. 57, no. 4, pp. 2342–2359, 2011.
- [45] Z. Zhu, Q. Li, G. Tang, and M. B. Wakin, "Global optimality in low-rank matrix optimization," *IEEE Transactions on Signal Processing*, vol. 66, no. 13, pp. 3614–3628, 2018.
- [46] C. Ma, Y. Li, and Y. Chi, "Beyond procrustes: Balancing-free gradient descent for asymmetric low-rank matrix sensing," *IEEE Transactions on Signal Processing*, vol. 69, pp. 867–877, 2021.
- [47] Z. Zhu, Q. Li, G. Tang, and M. B. Wakin, "The global optimization geometry of low-rank matrix optimization," *IEEE Transactions on Information Theory*, vol. 67, no. 2, pp. 1308–1331, 2021.
- [48] Z. Qin, M. B. Wakin, and Z. Zhu, "Guaranteed nonconvex factorization approach for tensor train recovery," *arXiv preprint arXiv:2401.02592*, 2024.
- [49] Z. Qin and Z. Zhu, "Robust low-rank tensor train recovery," *arXiv preprint arXiv:2410.15224*, 2024.
- [50] S. Holtz, T. Rohwedder, and R. Schneider, "On manifolds of tensors of fixed TT-rank," *Numerische Mathematik*, vol. 120, no. 4, pp. 701–731, 2012.
- [51] B. Li, Z. Zhang, Z. Hu, and Y. Chen, "Joint array diagnosis and channel estimation for ris-aided mmwave mimo system," *IEEE Access*, vol. 8, pp. 193 992–194 006, 2020.
- [52] Y. Lin, S. Jin, M. Matthaiou, and X. You, "Tensor-based algebraic channel estimation for hybrid ris-assisted mimo-ofdm," *IEEE Transactions on Wireless Communications*, vol. 20, no. 6, pp. 3770–3784, 2021.
- [53] A. Cichocki, "Tensor networks for big data analytics and large-scale optimization problems," *arXiv preprint arXiv:1407.3124*, 2014.
- [54] D. L. Donoho, "Compressed sensing," *IEEE Transactions on information theory*, vol. 52, no. 4, pp. 1289–1306, 2006.
- [55] E. J. Candès, J. Romberg, and T. Tao, "Robust uncertainty principles: Exact signal reconstruction from highly incomplete frequency information," *IEEE Transactions on information theory*, vol. 52, no. 2, pp. 489–509, 2006.
- [56] E. J. Candès and M. B. Wakin, "An introduction to compressive sampling," *IEEE signal processing magazine*, vol. 25, no. 2, pp. 21–30, 2008.
- [57] H. Rauhut, R. Schneider, and Ž. Stojanac, "Low rank tensor recovery via iterative hard thresholding," *Linear Algebra and its Applications*, vol. 523, pp. 220–262, 2017.

- [58] Z. Qin and Z. Zhu, "Computational and statistical guarantees for tensor-on-tensor regression with tensor train decomposition," *arXiv preprint arXiv:2406.06002*, 2024.
- [59] B. Recht, M. Fazel, and P. A. Parrilo, "Guaranteed minimum-rank solutions of linear matrix equations via nuclear norm minimization," *SIAM review*, vol. 52, no. 3, pp. 471–501, 2010.
- [60] J. Li, J. Wang, X. Wang, G. Qiao, H. Luo, and T. A. Gulliver, "Optimal beamforming design for underwater acoustic communication with multiple unsteady sub-gaussian interferers," *IEEE Transactions on Vehicular Technology*, vol. 68, no. 12, pp. 12 381–12 386, 2019.
- [61] J.-T. Yuan and K.-D. Tsai, "Analysis of the multimodulus blind equalization algorithm in qam communication systems," *IEEE Transactions on Communications*, vol. 53, no. 9, pp. 1427–1431, 2005.
- [62] L. Huang, J. Zhang, L. Zhang, and Z. Ye, "Widely linear minimum dispersion beamforming for sub-gaussian noncircular signals," *Signal Processing*, vol. 122, pp. 123–128, 2016.
- [63] R. W. Heath, N. Gonzalez-Prelcic, S. Rangan, W. Roh, and A. M. Sayeed, "An overview of signal processing techniques for millimeter wave mimo systems," *IEEE journal of selected topics in signal processing*, vol. 10, no. 3, pp. 436–453, 2016.
- [64] E. J. Candes and Y. Plan, "Tight oracle inequalities for low-rank matrix recovery from a minimal number of noisy random measurements," *IEEE Transactions on Information Theory*, vol. 57, no. 4, pp. 2342–2359, 2011.
- [65] L. Dai, B. Wang, M. Wang, X. Yang, J. Tan, S. Bi, S. Xu, F. Yang, Z. Chen, M. Di Renzo *et al.*, "Reconfigurable intelligent surface-based wireless communications: Antenna design, prototyping, and experimental results," *IEEE access*, vol. 8, pp. 45 913–45 923, 2020.
- [66] C. Huang, S. Hu, G. C. Alexandropoulos, A. Zappone, C. Yuen, R. Zhang, M. Di Renzo, and M. Debbah, "Holographic mimo surfaces for 6g wireless networks: Opportunities, challenges, and trends," *IEEE Wireless Communications*, vol. 27, no. 5, pp. 118–125, 2020.
- [67] W. Saad, M. Bennis, and M. Chen, "A vision of 6g wireless systems: Applications, trends, technologies, and open research problems," *IEEE network*, vol. 34, no. 3, pp. 134–142, 2019.
- [68] K. B. Letaief, W. Chen, Y. Shi, J. Zhang, and Y.-J. A. Zhang, "The roadmap to 6g: Ai empowered wireless networks," *IEEE communications magazine*, vol. 57, no. 8, pp. 84–90, 2019.
- [69] C. Huang, Z. Yang, G. C. Alexandropoulos, K. Xiong, L. Wei, C. Yuen, Z. Zhang, and M. Debbah, "Multi-hop ris-empowered terahertz communications: A drl-based hybrid beamforming design," *IEEE Journal on Selected Areas in Communications*, vol. 39, no. 6, pp. 1663–1677, 2021.
- [70] K. Ardah, S. Gherekhloo, A. L. de Almeida, and M. Haardt, "Double-ris versus single-ris aided systems: Tensor-based mimo channel estimation and design perspectives," in *ICASSP 2022-2022 IEEE International Conference on Acoustics, Speech and Signal Processing (ICASSP)*. IEEE, 2022, pp. 5183–5187.
- [71] F. Xu, J. Yao, W. Lai, K. Shen, X. Li, X. Chen, and Z.-Q. Luo, "Coordinating multiple intelligent reflecting surfaces without channel information," *arXiv preprint arXiv:2302.09717*, 2023.
- [72] N. D. Sidiropoulos, G. B. Giannakis, and R. Bro, "Blind parafac receivers for ds-cdma systems," *IEEE Transactions on Signal Processing*, vol. 48, no. 3, pp. 810–823, 2000.
- [73] G. Favier and A. L. de Almeida, "Tensor space-time-frequency coding with semi-blind receivers for mimo wireless communication systems," *IEEE Transactions on Signal Processing*, vol. 62, no. 22, pp. 5987–6002, 2014.
- [74] Í. V. Cavalcante, A. L. de Almeida, and M. Haardt, "Joint channel estimation for three-hop mimo relaying systems," *IEEE Signal Processing Letters*, vol. 22, no. 12, pp. 2430–2434, 2015.
- [75] G. Favier, C. A. R. Fernandes, and A. L. de Almeida, "Nested tucker tensor decomposition with application to mimo relay systems using tensor space-time coding (tstc)," *Signal Processing*, vol. 128, pp. 318–331, 2016.
- [76] J.-F. Cai, J. Li, and D. Xia, "Provable tensor-train format tensor completion by riemannian optimization," *Journal of Machine Learning Research*, vol. 23, no. 123, pp. 1–77, 2022.
- [77] P. Jain, R. Meka, and I. Dhillon, "Guaranteed rank minimization via singular value projection," *Advances in Neural Information Processing Systems*, vol. 23, 2010.
- [78] D. V. Savostyanov, "Quasioptimality of maximum-volume cross interpolation of tensors," *Linear Algebr. Appl.*, vol. 458, no. 1, pp. 217–244, Oct. 2014.
- [79] Z. Qin, A. Lidiak, Z. Gong, G. Tang, M. B. Wakin, and Z. Zhu, "Error analysis of tensor-train cross approximation," *Advances in Neural Information Processing Systems*, vol. 35, pp. 14 236–14 249, 2022.
- [80] B. Zheng, C. You, and R. Zhang, "Double-irs assisted multi-user mimo: Cooperative passive beamforming design," *IEEE Transactions on Wireless Communications*, vol. 20, no. 7, pp. 4513–4526, 2021.
- [81] Y. Han, S. Zhang, L. Duan, and R. Zhang, "Double-irs aided mimo communication under los channels: Capacity maximization and scaling," *IEEE Transactions on Communications*, vol. 70, no. 4, pp. 2820–2837, 2022.
- [82] H. A. Le, T. Van Chien, W. Choi *et al.*, "Double ris-assisted mimo systems over spatially correlated rician fading channels and finite scatterers," *IEEE Transactions on Communications*, 2023.
- [83] A. Zhang and D. Xia, "Tensor svd: Statistical and computational limits," *IEEE Transactions on Information Theory*, vol. 64, no. 11, pp. 7311–7338, 2018.
- [84] Y. Luo and A. R. Zhang, "Tensor-on-tensor regression: Riemannian optimization, over-parameterization, statistical-computational gap, and their interplay," *arXiv preprint arXiv:2206.08756*, 2022.
- [85] A. Agarwal, S. Negahban, and M. J. Wainwright, "Noisy matrix decomposition via convex relaxation: Optimal rates in high dimensions," *The Annals of Statistics*, vol. 40, no. 2, pp. 1171–1197, 2012.

## APPENDIX A

### INTRODUCTION OF THE TT DECOMPOSITION

For an order- $D$  tensor  $\mathcal{B} \in \mathbb{C}^{N_1 \times \dots \times N_D}$ , the  $(s_1, \dots, s_D)$ -th element of  $\mathcal{B}$  in the TT format can be expressed as the following matrix product form [37]

$$\mathcal{B}(s_1, \dots, s_D) = \mathbf{B}_1(:, s_1, :) \mathbf{B}_2(:, s_2, :) \cdots \mathbf{B}_D(:, s_D, :), \quad (29)$$

where tensor factors  $\mathbf{B}_d \in \mathbb{C}^{r_{d-1} \times N_d \times r_d}$ ,  $d = 1, \dots, D$  with  $r_0 = r_D = 1$ . Thus, the TT format can be represented by  $D$  tensor factors  $\{\mathbf{B}_d\}_{d \geq 1}$ , with a total of  $O(D\bar{N}\bar{r}^2)$  parameters, where  $\bar{N} = \max_d N_d$  and  $\bar{r} = \max_d r_d$ . In addition, for any two TT format tensors  $\tilde{\mathcal{B}}, \hat{\mathcal{B}} \in \mathbb{C}^{N_1 \times \dots \times N_D}$  with factors  $\{\tilde{\mathbf{B}}_d(s_d) \in \mathbb{C}^{\tilde{r}_{d-1} \times \tilde{r}_d}\}$  and  $\{\hat{\mathbf{B}}_d(s_d) \in \mathbb{C}^{\hat{r}_{d-1} \times \hat{r}_d}\}$ , each element of the summation  $\mathcal{B} = \tilde{\mathcal{B}} + \hat{\mathcal{B}}$  can be represented by

$$\mathcal{B}(s_1, \dots, s_D) = \begin{bmatrix} \tilde{\mathbf{B}}_1(s_1) & \hat{\mathbf{B}}_1(s_1) \end{bmatrix} \begin{bmatrix} \tilde{\mathbf{B}}_2(s_2) & \mathbf{0} \\ \mathbf{0} & \hat{\mathbf{B}}_2(s_2) \end{bmatrix} \cdots \begin{bmatrix} \tilde{\mathbf{B}}_{D-1}(s_{D-1}) & \mathbf{0} \\ \mathbf{0} & \hat{\mathbf{B}}_{D-1}(s_{D-1}) \end{bmatrix} \begin{bmatrix} \tilde{\mathbf{B}}_D(s_D) \\ \hat{\mathbf{B}}_D(s_D) \end{bmatrix}, \quad (30)$$

which implies that  $\mathcal{B}$  can also be represented in the TT format with ranks  $r_d \leq \tilde{r}_d + \hat{r}_d$  for  $d = 1, \dots, D - 1$ .

Since any tensor can be decomposed in the TT format (29) with sufficiently large TT ranks [37, Theorem 2.1], the decomposition of a tensor  $\mathcal{B}$  into the form (29) is generally not unique: not only are the factors  $\mathbf{B}_d(:, s_d, :)$  not unique, but also the dimensions of these factors can vary. To introduce the factorization with the smallest possible dimensions  $\mathbf{r} = (r_1, \dots, r_{D-1})$ , for convenience, for each  $d$ , we put  $\{\mathbf{B}_d(:, s_d, :)\}_{s_d=1}^{N_d}$  together into the following two forms

$$L(\mathbf{B}_d) = \begin{bmatrix} \mathbf{B}_d(1) \\ \vdots \\ \mathbf{B}_d(N_d) \end{bmatrix} \in \mathbb{C}^{(r_{d-1}N_d) \times r_d}, \quad (31)$$

$$R(\mathbf{B}_d) = [\mathbf{B}_d(1) \cdots \mathbf{B}_d(N_d)] \in \mathbb{C}^{r_{d-1} \times (N_d r_d)}, \quad (32)$$

where  $L(\mathbf{B}_d)$  and  $R(\mathbf{B}_d)$  are often called the left and right unfoldings of  $\mathbf{B}_d$ , respectively, if we view  $\mathbf{B}_d$  as a tensor. We say the decomposition (29) is minimal if the rank of the left unfolding matrix  $L(\mathbf{B}_d)$  is  $r_d$  and the rank of the right unfolding matrix  $R(\mathbf{B}_d)$  is  $r_{d-1}$  for all  $d$ . The dimensions  $\mathbf{r} =$

$(r_1, \dots, r_{D-1})$  of such a minimal decomposition are called the TT ranks of  $\mathcal{B}$ . According to [50], there is exactly one set of ranks  $\mathbf{r}$  that  $\mathcal{B}$  admits a minimal TT decomposition.

#### APPENDIX B PROOF OF THEOREM 1

*Proof.* By substituting the concentration inequality from [64, Theorem 2.3] with the concentration inequality for complex-valued subgaussian random variables, when (9) holds true, we can assert with a probability of  $1 - e^{-cT}$  that:

$$(1 - \delta_{UM}) \|\mathcal{B}(p, k, :)\|_F^2 \leq \frac{1}{T} \|\mathcal{X}(\mathcal{B})(p, k, :)\|_2^2 \leq (1 + \delta_{UM}) \|\mathcal{B}(p, k, :)\|_F^2. \quad (33)$$

Due to  $\|\mathcal{X}(\mathcal{B})\|_F^2 = \sum_{p,k} \|\mathcal{X}(\mathcal{B})(p, k, :)\|_2^2$  and  $\|\mathcal{B}\|_F^2 = \sum_{p,k} \|\mathcal{B}(p, k, :)\|_F^2$ , this completes the proof.  $\square$

#### APPENDIX C PROOF OF THEOREM 2

*Proof.* Using (7), we have

$$\begin{aligned} 0 &\leq \frac{1}{T} \|\mathcal{X}(\mathcal{B}^*) - \mathcal{Y}\|_F^2 - \frac{1}{T} \|\mathcal{X}(\widehat{\mathcal{B}}) - \mathcal{Y}\|_F^2 \\ &= \frac{1}{T} \|\mathcal{X}(\mathcal{B}^*) - \mathcal{X}(\widehat{\mathcal{B}}) - \mathcal{W}\|_F^2 \\ &\quad - \frac{1}{T} \|\mathcal{X}(\widehat{\mathcal{B}}) - \mathcal{X}(\mathcal{B}^*) - \mathcal{W}\|_F^2 \\ &= \frac{2}{T} \operatorname{Re} \left\{ \langle \mathcal{X}(\mathcal{B}^*) + \mathcal{W}, \mathcal{X}(\widehat{\mathcal{B}} - \mathcal{B}^*) \rangle \right\} \\ &\quad + \frac{1}{T} \|\mathcal{X}(\mathcal{B}^*)\|_F^2 - \frac{1}{T} \|\mathcal{X}(\widehat{\mathcal{B}})\|_F^2 \\ &= \frac{2}{T} \operatorname{Re} \left\{ \langle \mathcal{W}, \mathcal{X}(\widehat{\mathcal{B}} - \mathcal{B}^*) \rangle \right\} - \frac{1}{T} \|\mathcal{X}(\widehat{\mathcal{B}} - \mathcal{B}^*)\|_F^2, \end{aligned} \quad (34)$$

which further implies that

$$\frac{1}{T} \|\mathcal{X}(\widehat{\mathcal{B}} - \mathcal{B}^*)\|_F^2 \leq \frac{2}{T} |\langle \mathcal{W}, \mathcal{X}(\widehat{\mathcal{B}} - \mathcal{B}^*) \rangle|. \quad (35)$$

According to (11), we can directly obtain

$$\frac{1}{T} \|\mathcal{X}(\widehat{\mathcal{B}} - \mathcal{B}^*)\|_F^2 \geq (1 - \delta_{UM}) \|\widehat{\mathcal{B}} - \mathcal{B}^*\|_F^2. \quad (36)$$

For the right-hand side of (35), a straightforward application of the Cauchy-Schwarz inequality  $|\langle \mathcal{W}, \mathcal{X}(\widehat{\mathcal{B}} - \mathcal{B}^*) \rangle| \leq \|\mathcal{W}\|_F \|\mathcal{X}(\widehat{\mathcal{B}} - \mathcal{B}^*)\|_F$  is not adequate to fully elucidate the interplay of all parameters. We address this issue by using the covering argument to bound  $|\langle \mathcal{W}, \mathcal{X}(\widehat{\mathcal{B}} - \mathcal{B}^*) \rangle|$  for all possible  $\mathcal{B}$ .

Now, we rewrite  $\frac{2}{T} |\langle \mathcal{W}, \mathcal{X}(\widehat{\mathcal{B}} - \mathcal{B}^*) \rangle|$  as following:

$$\begin{aligned} &\frac{2}{T} |\langle \mathcal{W}, \mathcal{X}(\widehat{\mathcal{B}} - \mathcal{B}^*) \rangle| \\ &= \frac{2 \|\widehat{\mathcal{B}} - \mathcal{B}^*\|_F}{T} \max_{\mathcal{H} \in \mathbb{B}_{2N, S}, \|\mathcal{H}\|_F \leq 1} |\langle \mathcal{H}, \mathcal{W} \times_3^2 \mathbf{X}^* \rangle| \\ &= \frac{2 \|\widehat{\mathcal{B}} - \mathcal{B}^*\|_F}{T} \max_{\substack{\|\mathbf{H}_1\| \leq 1, \|\mathbf{H}_2\|_F \leq 1, \\ \|\mathcal{L}(\widetilde{\mathcal{S}})\| \leq 1}} |\langle [\mathbf{H}_1, \widetilde{\mathcal{S}}, \mathbf{H}_2], \mathcal{W} \times_3^2 \mathbf{X}^* \rangle|, \end{aligned} \quad (37)$$

where  $\mathbf{X}^*$  is the conjugate matrix of  $\mathbf{X}$  and  $\mathcal{W} \times_3^2 \mathbf{X}^* = \sum_{t=1}^T \mathcal{W}(:, :, t) \mathbf{X}^*(:, t)$ . According to [48, eq.(44)], the last

line follows  $\|\mathcal{H}\|_F = \|\mathbf{H}_2\|_F \leq 1$  for a left-orthogonal TT form in Appendix A.

To begin, according to [83], we can construct an  $\epsilon$ -net  $\{\mathbf{H}_1^{(1)}, \dots, \mathbf{H}_1^{(n_1)}\}$  with the covering number  $n_1 \leq \left(\frac{4+\epsilon}{\epsilon}\right)^{LPN}$  for the set of factors  $\{\mathbf{H}_1 \in \mathbb{C}^{LP \times N} : \|\mathbf{H}_1\| \leq 1\}$  such that

$$\sup_{\mathbf{H}_1 : \|\mathbf{H}_1\| \leq 1} \min_{p_1 \leq n_1} \|\mathbf{H}_1 - \mathbf{H}_1^{(p_1)}\| \leq \epsilon. \quad (38)$$

Similarly, we can construct  $\epsilon$ -net  $\{\mathbf{H}_2^{(1)}, \dots, \mathbf{H}_2^{(n_2)}\}$  with the covering number  $n_2 \leq \left(\frac{2+\epsilon}{\epsilon}\right)^{UMN}$  for  $\{\mathbf{H}_2 \in \mathbb{C}^{N \times UM} : \|\mathbf{H}_2\|_F \leq 1\}$  such that

$$\sup_{\mathbf{H}_2 : \|\mathbf{H}_2\|_F \leq 1} \min_{p_2 \leq n_2} \|\mathbf{H}_2 - \mathbf{H}_2^{(p_2)}\|_F \leq \epsilon. \quad (39)$$

Therefore, we can construct an  $\epsilon$ -net  $\{\mathcal{H}^{(1)}, \dots, \mathcal{H}^{(n_1 n_2)}\}$  with covering number

$$n_1 n_2 \leq \left(\frac{4+\epsilon}{\epsilon}\right)^{LPN+UMN} \quad (40)$$

for any TT format tensor  $\mathcal{H} = [\mathbf{H}_1, \widetilde{\mathcal{S}}, \mathbf{H}_2] \in \mathbb{B}_{2N, \widetilde{\mathcal{S}}}$ .

Denote by  $A$  the value of (37), i.e.,

$$[\widetilde{\mathbf{H}}_1, \widetilde{\mathcal{S}}, \widetilde{\mathbf{H}}_2] = \arg \max_{\substack{\|\mathbf{H}_1\| \leq 1, \|\mathbf{H}_2\|_F \leq 1, \\ \|\mathcal{L}(\widetilde{\mathcal{S}})\| \leq 1}} 1/T |\langle [\mathbf{H}_1, \widetilde{\mathcal{S}}, \mathbf{H}_2], \mathcal{W} \times_3^2 \mathbf{X}^* \rangle|, \quad (41)$$

$$A := \frac{1}{T} |\langle [\widetilde{\mathbf{H}}_1, \widetilde{\mathcal{S}}, \widetilde{\mathbf{H}}_2], \mathcal{W} \times_3^2 \mathbf{X}^* \rangle|. \quad (42)$$

Using  $\mathcal{I}$  to denote the index set  $[n_1] \times [n_2]$ , then according to the construction of the  $\epsilon$ -net, there exists  $p = (p_1, p_2) \in \mathcal{I}$  such that

$$\|\widetilde{\mathbf{H}}_1 - \mathbf{H}_1^{(p_1)}\| \leq \epsilon, \quad \text{and} \quad \|\widetilde{\mathbf{H}}_2 - \mathbf{H}_2^{(p_2)}\|_F \leq \epsilon, \quad (43)$$

and taking  $\epsilon = \frac{1}{4}$  gives

$$\begin{aligned} A &\leq \frac{1}{T} |\langle [\mathbf{H}_1^{(p_1)}, \widetilde{\mathcal{S}}, \mathbf{H}_2^{(p_2)}], \mathcal{W} \times_3^2 \mathbf{X}^* \rangle| \\ &\quad + \frac{1}{T} |\langle [\widetilde{\mathbf{H}}_1, \widetilde{\mathcal{S}}, \widetilde{\mathbf{H}}_2] - [\mathbf{H}_1^{(p_1)}, \widetilde{\mathcal{S}}, \mathbf{H}_2^{(p_2)}], \mathcal{W} \times_3^2 \mathbf{X}^* \rangle| \\ &= \frac{1}{T} |\langle [\mathbf{H}_1^{(p_1)}, \widetilde{\mathcal{S}}, \mathbf{H}_2^{(p_2)}], \mathcal{W} \times_3^2 \mathbf{X}^* \rangle| \\ &\quad + \frac{1}{T} |\langle [\widetilde{\mathbf{H}}_1 - \mathbf{H}_1^{(p_1)}, \widetilde{\mathcal{S}}, \widetilde{\mathbf{H}}_2] \\ &\quad + [\mathbf{H}_1^{(p_1)}, \widetilde{\mathcal{S}}, \widetilde{\mathbf{H}}_2 - \mathbf{H}_2^{(p_2)}], \mathcal{W} \times_3^2 \mathbf{X}^* \rangle| \\ &\leq \frac{1}{T} |\langle [\mathbf{H}_1^{(p_1)}, \widetilde{\mathcal{S}}, \mathbf{H}_2^{(p_2)}], \mathcal{W} \times_3^2 \mathbf{X}^* \rangle| + 2\epsilon A \\ &= \frac{1}{T} |\langle [\mathbf{H}_1^{(p_1)}, \widetilde{\mathcal{S}}, \mathbf{H}_2^{(p_2)}], \mathcal{W} \times_3^2 \mathbf{X}^* \rangle| + \frac{A}{2}. \end{aligned} \quad (44)$$

Note that each element in  $\mathcal{W}$  follows the complex normal distribution  $\mathcal{CN}(0, \gamma^2)$ . When conditional on  $\mathbf{X}$ , for any fixed  $\mathcal{H}^{(p)} = [\mathbf{H}_1^{(p_1)}, \widetilde{\mathcal{S}}, \mathbf{H}_2^{(p_2)}] \in \mathbb{C}^{LP \times K \times UM}$ ,  $\frac{1}{T} \langle \mathcal{H}^{(p)}, \mathcal{W} \times_3^2 \mathbf{X}^* \rangle$  has complex normal distribution with zero mean and variance  $\frac{\gamma^2 \|\mathcal{X}(\mathcal{H}^{(p)})\|_F^2}{T^2}$ , which implies that

$$\mathbb{P} \left( \frac{1}{T} |\langle \mathcal{H}^{(p)}, \mathcal{W} \times_3^2 \mathbf{X}^* \rangle| \geq t \mid \mathbf{X} \right) \leq e^{-\frac{T^2 t^2}{2\gamma^2 \|\mathcal{X}(\mathcal{H}^{(p)})\|_F^2}}. \quad (45)$$

Furthermore, under the event  $F := \{\mathcal{X} \text{ satisfies } UM\text{-RIP with constant } \delta_{UM}\}$ , which implies that  $\frac{1}{T} \|\mathcal{X}(\mathcal{H}^{(p)})\|_F^2 \leq$

$(1 + \delta_{UM})\|\mathcal{H}^{(p)}\|_F^2$ . Plugging this together with the fact  $\|\mathcal{H}^{(p)}\|_F \leq 1$  into the above further gives

$$\mathbb{P}\left(\frac{1}{T}|\langle \mathcal{H}^{(p)}, \mathcal{W} \times_3^2 \mathbf{X}^* \rangle| \geq t|F\right) \leq e^{-\frac{Tt^2}{2(1+\delta_{UM})\gamma^2}}. \quad (46)$$

We now apply this tail bound to (44) and get

$$\begin{aligned} \mathbb{P}(A \geq t|F) &\leq \mathbb{P}\left(\max_{p_1, p_2} \frac{1}{T}|\langle \mathcal{H}^{(p)}, \mathcal{W} \times_3^2 \mathbf{X}^* \rangle| \geq \frac{t}{2}|F\right) \\ &\leq \left(\frac{4+\epsilon}{\epsilon}\right)^{2LPN+2UMN} e^{-\frac{Tt^2}{8(1+\delta_{UM})\gamma^2}} \\ &\leq e^{-\frac{Tt^2}{8(1+\delta_{UM})\gamma^2} + c_1(LP N + UM N)}, \end{aligned} \quad (47)$$

where  $c_1$  is a constant and based on the assumption  $\epsilon = \frac{1}{4}$  in (44),  $\frac{4+\epsilon}{\epsilon} = 17$ .

Hence, we can take  $t = \frac{c_2\sqrt{(1+\delta_{UM})(LPN+UMN)}}{\sqrt{T}}\gamma$  with a constant  $c_2$  and further derive

$$\begin{aligned} &\mathbb{P}\left(A \leq \frac{c_2\sqrt{(1+\delta_{UM})(LPN+UMN)}}{\sqrt{T}}\gamma\right) \\ &\geq \mathbb{P}\left(A \leq \frac{c_2\sqrt{(1+\delta_{UM})(LPN+UMN)}}{\sqrt{T}}\gamma \cap F\right) \\ &\geq P(F)\mathbb{P}\left(A \leq \frac{c_2\sqrt{(1+\delta_{UM})(LPN+UMN)}}{\sqrt{T}}\gamma|F\right) \\ &\geq (1 - e^{-c_3UM})(1 - e^{-c_4(LP N + UM N)}) \\ &\geq 1 - 2e^{-c_5(LP N + UM N)}, \end{aligned} \quad (48)$$

where  $c_i, i = 3, 4, 5$  are constants. Note that  $P(F)$  follows Theorem 1.

Combing (36), we can obtain

$$\|\widehat{\mathcal{B}} - \mathcal{B}^*\|_F \leq O\left(\frac{\gamma\sqrt{(1+\delta_{UM})(LPN+UMN)}}{(1-\delta_{UM})\sqrt{T}}\right). \quad (49)$$

□

#### APPENDIX D PROOF OF THEOREM 3

*Proof.* Suppose we can find a set of  $\{\mathcal{B}^j\}_{j=1}^n \in \mathbb{B}_{N,S}$  such that  $\min_{j \neq k} \|\mathcal{B}^j - \mathcal{B}^k\|_F \geq s$ . According to [84, Theorem 4], when each element of  $\mathbf{X}$  and  $\mathcal{W}$  respectively follow  $\mathcal{CN}(0, 1)$  and  $\mathcal{CN}(0, \gamma^2)$ , we have

$$\begin{aligned} &\inf_{\widehat{\mathcal{B}}} \sup_{\mathcal{B} \in \mathbb{B}_{N,S}} \mathbb{E} \|\widehat{\mathcal{B}} - \mathcal{B}\|_F \\ &\geq \frac{s}{2} \left(1 - \frac{T}{2\gamma^2} \max_{j_1 \neq j_2} \|\mathcal{B}^{j_1} - \mathcal{B}^{j_2}\|_F^2 + \log 2\right). \end{aligned} \quad (50)$$

Next, we consider one construction for the sets of  $\{\mathcal{B}^j\}_{j=1}^n \in \mathbb{B}_{N,S}$  such that we can obtain a proper lower bound for  $\min_{j_1 \neq j_2} \|\mathcal{B}^{j_1} - \mathcal{B}^{j_2}\|_F$  and a proper upper bound for  $\max_{j_1 \neq j_2} \|\mathcal{B}^{j_1} - \mathcal{B}^{j_2}\|_F$ . Given the equivalence between any two tensors  $\mathcal{B}^{j_1} = [\mathbf{A}_1^{j_1}, \mathcal{S}, \mathbf{A}_2]$ ,  $\mathcal{B}^{j_2} = [\mathbf{A}_1^{j_2}, \mathcal{S}, \mathbf{A}_2]$  and their canonical forms [48], the TT-SVD can be applied to transform these tensors into canonical formats  $\widehat{\mathcal{B}}^{j_1} = [\widehat{\mathbf{A}}_1^{j_1}, \widehat{\mathcal{S}}, \widehat{\mathbf{A}}_2]$  and  $\widehat{\mathcal{B}}^{j_2} = [\widehat{\mathbf{A}}_1^{j_2}, \widehat{\mathcal{S}}, \widehat{\mathbf{A}}_2]$  with  $R(\widehat{\mathcal{S}})R^H(\widehat{\mathcal{S}}) = \mathbf{I}_N$  and  $\widehat{\mathbf{A}}_2 \widehat{\mathbf{A}}_2^H = \mathbf{I}_N$ . Given any  $\delta > 0$  and  $N \geq C'$  by

[85, Lemma 5], we can construct a set of  $\{\widehat{\mathbf{A}}_1^1, \dots, \widehat{\mathbf{A}}_1^{n_0}\}$  with cardinality  $n_0 \geq \frac{1}{4}e^{\frac{LPN}{128}}$  such that: (1)  $\|\widehat{\mathbf{A}}_1^j\|_F = \delta$  holds for all  $j = 1, \dots, n_0$ , (2)  $\|\widehat{\mathbf{A}}_1^{j_1} - \widehat{\mathbf{A}}_1^{j_2}\|_F \geq \delta$  for all  $j_1, j_2 \in [n_0], j_1 \neq j_2$ .

Due to  $\|\mathcal{B}^{j_1} - \mathcal{B}^{j_2}\|_F = \|[\widehat{\mathbf{A}}_1^{j_1} - \widehat{\mathbf{A}}_1^{j_2}, \widehat{\mathcal{S}}, \widehat{\mathbf{A}}_2]\|_F = \|\widehat{\mathbf{A}}_1^{j_1} - \widehat{\mathbf{A}}_1^{j_2}\|_F$ , we can further get

$$\begin{aligned} \max_{j_1 \neq j_2} \|\mathcal{B}^{j_1} - \mathcal{B}^{j_2}\|_F &= \max_{j_1 \neq j_2} \|\widehat{\mathbf{A}}_1^{j_1} - \widehat{\mathbf{A}}_1^{j_2}\|_F \leq 2\delta, \\ \min_{j_1 \neq j_2} \|\mathcal{B}^{j_1} - \mathcal{B}^{j_2}\|_F &= \min_{j_1 \neq j_2} \|\widehat{\mathbf{A}}_1^{j_1} - \widehat{\mathbf{A}}_1^{j_2}\|_F \geq \delta. \end{aligned} \quad (51)$$

Then we plug (51) into (50) and have

$$\begin{aligned} \inf_{\widehat{\mathcal{B}}} \sup_{\mathcal{B} \in \mathbb{B}_{N,S}} \mathbb{E} \|\widehat{\mathcal{B}} - \mathcal{B}\|_F &\geq \frac{\delta}{2} \left(1 - \frac{2T\delta^2}{\gamma^2} + \log 2\right) \\ &\geq c_2 \sqrt{\frac{LPN}{T}}\gamma, \end{aligned} \quad (52)$$

where the second inequality with a constant  $c_2 > 0$  follows  $\delta = c_3\sqrt{\frac{LPN}{m}}\gamma$  for a constant  $c_3 > 0$ .

Similarly, we can utilize the TT-SVD to transform  $\mathcal{B}^{j_1} = [\mathbf{A}_1^{j_1}, \mathcal{S}, \mathbf{A}_2]$  and  $\mathcal{B}^{j_2} = [\mathbf{A}_1^{j_2}, \mathcal{S}, \mathbf{A}_2]$  into orthonormal formats  $\mathcal{B}^{j_1} = [\widetilde{\mathbf{A}}_1, \widetilde{\mathcal{S}}, \widetilde{\mathbf{A}}_2^{j_1}]$  and  $\mathcal{B}^{j_2} = [\widetilde{\mathbf{A}}_1, \widetilde{\mathcal{S}}, \widetilde{\mathbf{A}}_2^{j_2}]$  with  $L^H(\widetilde{\mathcal{S}})L(\widetilde{\mathcal{S}}) = \mathbf{I}_N$  and  $\widetilde{\mathbf{A}}_1^H \widetilde{\mathbf{A}}_1 = \mathbf{I}_N$ . Then following the previous analysis, we can get

$$\inf_{\widehat{\mathcal{B}}} \sup_{\mathcal{B} \in \mathbb{B}_{N,S}} \mathbb{E} \|\widehat{\mathcal{B}} - \mathcal{B}\|_F \geq \Omega\left(\sqrt{\frac{UMN}{T}}\gamma\right). \quad (53)$$

Finally, we sum (52)-(53) and calculate the average to derive

$$\inf_{\widehat{\mathcal{B}}} \sup_{\mathcal{B} \in \mathbb{B}_{N,S}} \mathbb{E} \|\widehat{\mathcal{B}} - \mathcal{B}\|_F \geq \Omega\left(\sqrt{\frac{LPN + UMN}{2T}}\gamma\right). \quad (54)$$

□

#### APPENDIX E PROOF OF THEOREM 5

*Proof.* Utilizing the identical derivation as (35), we can directly acquire

$$\frac{1}{T} \|\mathcal{X}(\widehat{\mathcal{B}}_D - \mathcal{B}_D^*)\|_F^2 \leq \frac{2}{T} |\langle \mathcal{W}, \mathcal{X}(\widehat{\mathcal{B}}_D - \mathcal{B}_D^*) \rangle|. \quad (55)$$

First, according to Theorem 4, we have

$$\frac{1}{T} \|\mathcal{X}(\widehat{\mathcal{B}}_D - \mathcal{B}_D^*)\|_F^2 \geq (1 - \delta_{UM}) \|\widehat{\mathcal{B}}_D - \mathcal{B}_D^*\|_F^2. \quad (56)$$

Additionally, we can also rewrite  $\frac{2}{T} |\langle \mathcal{W}, \mathcal{X}(\widehat{\mathcal{B}}_D - \mathcal{B}_D^*) \rangle|$  as follows:

$$\begin{aligned} &\frac{2}{T} |\langle \mathcal{W}, \mathcal{X}(\widehat{\mathcal{B}}_D - \mathcal{B}_D^*) \rangle| \\ &= \frac{2\|\widehat{\mathcal{B}}_D - \mathcal{B}_D^*\|_F}{T} \max_{\mathcal{H} \in \mathbb{B}_{2N}^D, \|\mathcal{H}\|_F \leq 1} |\langle \mathcal{H}, \mathcal{W} \times_3^2 \mathbf{X}^* \rangle| \\ &= \frac{2\|\widehat{\mathcal{B}}_D - \mathcal{B}_D^*\|_F}{T} \max_{\substack{\|\mathbf{H}_i\| \leq 1, i \in [D], \\ \|\mathcal{L}(\widetilde{\mathcal{S}}_i)\| \leq 1, i \in [D], \|\mathbf{H}_0\|_F \leq 1}} |\langle [\mathbf{H}_D, \widetilde{\mathcal{S}}_D, \dots, \mathbf{H}_0], \mathcal{W} \times_3^2 \mathbf{X}^* \rangle|. \end{aligned} \quad (57)$$

The last line follows that  $\|\mathcal{H}\|_F^2 = \|\mathbf{H}_0\|_F^2 \leq 1$  for a left-orthogonal TT form in Appendix A.

Next, we can construct an  $\epsilon$ -net  $\{\mathbf{H}_i^{(1)}, \dots, \mathbf{H}_i^{(n_i)}\}$  with the covering number  $n_i \leq \left(\frac{4+\epsilon}{\epsilon}\right)^{N_i N_{i+1}}$ ,  $i \in [D]$  for the set of factors  $\{\mathbf{H}_i \in \mathbb{C}^{N_{i+1} \times N_i} : \|\mathbf{H}_i\| \leq 1\}$  such that

$$\sup_{\mathbf{H}_i: \|\mathbf{H}_i\| \leq 1} \min_{p_i \leq n_i} \|\mathbf{H}_i - \mathbf{H}_i^{(p_i)}\| \leq \epsilon. \quad (58)$$

In addition, we can construct an  $\epsilon$ -net  $\{\mathbf{H}_0^{(1)}, \dots, \mathbf{H}_0^{(n_0)}\}$  with the covering number  $n_0 \leq \left(\frac{2+\epsilon}{\epsilon}\right)^{N_0 N_1}$  for the set of factors  $\{\mathbf{H}_0 \in \mathbb{C}^{N_1 \times N_0} : \|\mathbf{H}_0\|_F \leq 1\}$  such that

$$\sup_{\mathbf{H}_0: \|\mathbf{H}_0\|_F \leq 1} \min_{p_0 \leq n_0} \|\mathbf{H}_0 - \mathbf{H}_0^{(p_0)}\|_F \leq \epsilon. \quad (59)$$

Therefore, we can construct an  $\epsilon$ -net  $\{\mathcal{H}^{(1)}, \dots, \mathcal{H}^{(n_0 \cdots n_D)}\}$  with covering number

$$n_0 \cdots n_D \leq \left(\frac{4+\epsilon}{\epsilon}\right)^{\sum_{d=0}^D N_d N_{d+1}} \quad (60)$$

for any  $\mathcal{H} \in \mathbb{B}_{2N, \{\tilde{\mathcal{S}}_i\}}^D$ .

Denote by  $A$  the value of (57), i.e.,

$$\begin{aligned} & [\widetilde{\mathbf{H}}_D, \widetilde{\mathcal{S}}_D, \dots, \widetilde{\mathbf{H}}_1, \widetilde{\mathcal{S}}_1, \widetilde{\mathbf{H}}_0] \\ &= \arg \max_{\substack{\|\mathbf{H}_i\| \leq 1, i \in [D], \\ \|\mathcal{L}(\tilde{\mathcal{S}}_i)\| \leq 1, i \in [D], \|\mathbf{H}_0\|_F \leq 1}} |\langle [\mathbf{H}_D, \widetilde{\mathcal{S}}_D, \dots, \mathbf{H}_1, \widetilde{\mathcal{S}}_1, \mathbf{H}_0], \mathcal{W} \times \frac{2}{3} \mathbf{X}^* \rangle|, \quad (61) \\ & A := \frac{1}{T} |\langle [\widetilde{\mathbf{H}}_D, \widetilde{\mathcal{S}}_D, \dots, \widetilde{\mathbf{H}}_1, \widetilde{\mathcal{S}}_1, \widetilde{\mathbf{H}}_0], \mathcal{W} \times \frac{2}{3} \mathbf{X}^* \rangle|. \quad (62) \end{aligned}$$

Using  $\mathcal{I}$  to denote the index set  $[n_0] \times \dots \times [n_D]$ , then according to the construction of the  $\epsilon$ -net, there exists  $p = (p_0, \dots, p_D) \in \mathcal{I}$  such that

$$\|\widetilde{\mathbf{H}}_i - \mathbf{H}_i^{(p_i)}\| \leq \epsilon, i \in [D] \text{ and } \|\widetilde{\mathbf{H}}_0 - \mathbf{H}_0^{(p_0)}\|_F \leq \epsilon, \quad (63)$$

and taking  $\epsilon = \frac{1}{2(D+1)}$  gives

$$\begin{aligned} A &\leq \frac{1}{T} |\langle [\mathbf{H}_D^{(p_D)}, \widetilde{\mathcal{S}}_D, \dots, \widetilde{\mathcal{S}}_1, \mathbf{H}_0^{(p_0)}], \mathcal{W} \times \frac{2}{3} \mathbf{X}^* \rangle| \\ &\quad + \frac{1}{T} |\langle [\widetilde{\mathbf{H}}_D, \widetilde{\mathcal{S}}_D, \dots, \widetilde{\mathcal{S}}_1, \widetilde{\mathbf{H}}_0] \\ &\quad - [\mathbf{H}_D^{(p_D)}, \widetilde{\mathcal{S}}_D, \dots, \widetilde{\mathcal{S}}_1, \mathbf{H}_0^{(p_0)}], \mathcal{W} \times \frac{2}{3} \mathbf{X}^* \rangle| \\ &= \frac{1}{T} |\langle [\mathbf{H}_D^{(p_D)}, \widetilde{\mathcal{S}}_D, \dots, \widetilde{\mathcal{S}}_1, \mathbf{H}_0^{(p_0)}], \mathcal{W} \times \frac{2}{3} \mathbf{X}^* \rangle| \\ &\quad + \frac{1}{T} \left| \sum_{i=0}^D \left\langle [\mathbf{H}_D^{(p_D)}, \widetilde{\mathcal{S}}_D, \mathbf{H}_{D-1}^{(p_{D-1})}, \dots, \mathbf{H}_{i+1}^{(p_{i+1})}, \widetilde{\mathcal{S}}_{i+1}, \right. \right. \\ &\quad \left. \left. \widetilde{\mathbf{H}}_i - \mathbf{H}_i^{(p_i)}, \widetilde{\mathcal{S}}_i, \widetilde{\mathbf{H}}_{i-1}, \dots, \widetilde{\mathcal{S}}_1, \widetilde{\mathbf{H}}_0], \mathcal{W} \times \frac{2}{3} \mathbf{X}^* \right\rangle \right| \\ &\leq \frac{1}{T} |\langle [\mathbf{H}_D^{(p_D)}, \widetilde{\mathcal{S}}_D, \dots, \widetilde{\mathcal{S}}_1, \mathbf{H}_0^{(p_0)}], \mathcal{W} \times \frac{2}{3} \mathbf{X}^* \rangle| \\ &\quad + (D+1)\epsilon A \\ &= \frac{1}{T} |\langle [\mathbf{H}_D^{(p_D)}, \widetilde{\mathcal{S}}_D, \dots, \widetilde{\mathcal{S}}_1, \mathbf{H}_0^{(p_0)}], \mathcal{W} \times \frac{2}{3} \mathbf{X}^* \rangle| + \frac{A}{2}, \quad (64) \end{aligned}$$

where the first equation follows the fact that  $(l, k, u)$ -th element of  $[\widetilde{\mathbf{H}}_D, \widetilde{\mathcal{S}}_D, \dots, \widetilde{\mathcal{S}}_1, \widetilde{\mathbf{H}}_0] - [\mathbf{H}_D^{(p_D)}, \widetilde{\mathcal{S}}_D, \dots, \widetilde{\mathcal{S}}_1, \mathbf{H}_0^{(p_0)}]$  can be decomposed into  $\sum_{i=0}^D \mathbf{H}_D^{(p_D)}(l, :)\widetilde{\mathcal{S}}_D(:, k, :)\mathbf{H}_{D-1}^{(p_{D-1})} \dots \mathbf{H}_{i+1}^{(p_{i+1})}\widetilde{\mathcal{S}}_{i+1}(:, k, :)(\widetilde{\mathbf{H}}_i - \mathbf{H}_i^{(p_i)})\widetilde{\mathcal{S}}_i(:, k, :)\widetilde{\mathbf{H}}_{i-1}\widetilde{\mathcal{S}}_1(:, k, :)\widetilde{\mathbf{H}}_0(:, u)$ .

Based on the same analysis of (48), we can obtain

$$\begin{aligned} & \mathbb{P} \left( A \leq \frac{c_1 \sqrt{(1 + \delta_{UM}) (\sum_{d=1}^{D-1} N_d N_{d+1}) \log D}}{\sqrt{T}} \gamma \right) \\ & \geq 1 - 2e^{-c_2 (\sum_{d=1}^{D-1} N_d N_{d+1}) \log D}, \quad (65) \end{aligned}$$

where  $c_i, i = 1, 2$  are constants.

Combing (56), we arrive at

$$\begin{aligned} & \|\widehat{\mathcal{B}}_D - \mathcal{B}_D^*\|_F \\ & \leq O \left( \frac{\gamma \sqrt{(1 + \delta_{UM}) (\sum_{d=1}^{D-1} N_d N_{d+1}) \log D}}{(1 - \delta_{UM}) \sqrt{T}} \right). \quad (66) \end{aligned}$$

□